UNIVERSIDADE FEDERAL DE MINAS GERAIS
Instituto de Ciências Exatas
Programa de Pós-Graduação em Física

Luis Elvis Cano Fernández

STUDY OF MICROCAVITY-QUANTUM DOT INTERACTIONS: From Weak to Strong Coupling, Incoherent Pumping, and Magnetic Field Effects

Belo Horizonte
2024

Luis Elvis Cano Fernández

STUDY OF MICROCAVITY-QUANTUM DOT INTERACTIONS: From Weak to Strong Coupling, Incoherent Pumping, and Magnetic Field Effects

Tese apresentada ao Programa de Pós-Graduação em Física do Instituto de Ciências Exatas da Universidade Federal de Minas Gerais como requisito parcial para obtenção do título de Doutor em Ciências.

Orientador: Paulo Sérgio Soares Guimarães

Coorientador: José Maria Villas-Bôas

Belo Horizonte
2024

Dados Internacionais de Catalogação na Publicação (CIP)

C227s Cano Fernández, Luis Elvis.
Study of microcavity-quantum dot interactions: from weak to strong coupling, incoherent pumping, and magnetic field effects / Luis Elvis Cano Fernández. – 2024.
63 f. : il.

Orientador: Paulo Sérgio Soares Guimarães.
Coorientador: José Maria Villas Bôas.
Tese (doutorado) – Universidade Federal de Minas Gerais, Departamento de Física.
Bibliografia: f. 52-63.

1. Sistemas quânticos. 2. Decoerência. 3. Retificação. I. Título. II. Guimarães, Paulo Sérgio Soares. III. Villas Bôas, José Maria. IV. Universidade Federal de Minas Gerais, Departamento de Física.

CDU – 530.145 (043)

Ficha catalográfica elaborada por Romário Martins Ribeiro – CRB6 3595
Biblioteca Professor Manoel Lopes de Siqueira – Departamento de Física - UFMG

UNIVERSIDADE FEDERAL DE MINAS GERAIS

ATA

ATA DA SESSÃO DE ARGUIÇÃO DA 437ª TESE DO PROGRAMA DE PÓS-GRADUAÇÃO EM FÍSICA, DEFENDIDA POR LUIS ELVIS CANO FERNANDEZ orientado pelo professor Paulo Sérgio Soares Guimarães e coorientado pelo professor José Maria Villas-Bôas, para obtenção do grau de **DOUTOR EM CIÊNCIAS, área de concentração Física**. Às 14:00 horas de 13 de dezembro de dois mil e vinte e quatro reuniu-se a Comissão Examinadora, composta pelos professores **Paulo Sérgio Soares Guimarães** (Orientador - Departamento de Física/UFMG), **José Maria Villas-Bôas** (Coorientador - Instituto de Física/UFU), **Simone Silva Alexandre** (Departamento de Física/UFMG)**, Sebastião José Nascimento de Pádua** (Departamento de Física/UFMG), **Guilherme Monteiro Torelly** (Departamento de Engenharia Elétrica PUC/RJ) e **Liliana Sanz de la Torre** (Instituto de Física/UFU) para dar cumprimento ao Artigo 37 do Regimento Geral da UFMG, submetendo o Mestre **LUIS ELVIS CANO FERNANDEZ** à arguição de seu trabalho de tese de Doutorado, que recebeu o título de "**Study of Microcavity-Quantum Dot Interactions: From Weak to Strong Coupling, Incoherent Pumping, and Magnetic Field Effects**". O candidato fez uma exposição oral de seu trabalho durante aproximadamente 50 minutos. Após esta, os membros da comissão prosseguiram com a sua arguição, e apresentaram seus pareceres individuais sobre o trabalho, concluindo pela aprovação do candidato.

Belo Horizonte, 13 de dezembro de 2024

Paulo Sérgio Soares Guimarães
Orientador do estudante
Departamento de Física /UFMG

José Maria Villas-Bôas
Coorientador do estudante
Instituto de Física /UFU

Simone Silva Alexandre
Departamento de Física /UFMG

Sebastião José Nascimento de Pádua
Departamento de Física /UFMG

Guilherme Monteiro Torelly
Departamento de Engenharia Elétrica /PUC-RJ

Liliana Sanz de la Torre
Instituto de Física /UFU

Candidato: Luis Elvis Cano Fernandez

Documento assinado eletronicamente por **Liliana Sanz registrado(a) civilmente como Liliana Sanz de la Torre**, **Usuária Externa**, em 16/12/2024, às 17:26, conforme horário oficial de Brasília, com fundamento no art. 5º do Decreto nº 10.543, de 13 de novembro de 2020.

Documento assinado eletronicamente por **Guilherme Monteiro Torelly**, **Usuário Externo**, em 16/12/2024, às 18:10, conforme horário oficial de Brasília, com fundamento no art. 5º do Decreto nº 10.543, de 13 de novembro de 2020.

Documento assinado eletronicamente por **Paulo Sergio Soares Guimaraes**, **Professor do Magistério Superior**, em 16/12/2024, às 20:11, conforme horário oficial de Brasília, com fundamento no art. 5º do Decreto nº 10.543, de 13 de novembro de 2020.

Documento assinado eletronicamente por **José Maria Villas Bôas**, **Usuário Externo**, em 17/12/2024, às 17:15, conforme horário oficial de Brasília, com fundamento no art. 5º do Decreto nº 10.543, de 13 de novembro de 2020.

Documento assinado eletronicamente por **Luis Elvis Cano Fernandez**, **Usuário Externo**, em 19/12/2024, às 14:45, conforme horário oficial de Brasília, com fundamento no art. 5º do Decreto nº 10.543, de 13 de novembro de 2020.

Documento assinado eletronicamente por **Simone Silva Alexandre**, **Professora do Magistério Superior**, em 10/01/2025, às 11:26, conforme horário oficial de Brasília, com fundamento no art. 5º do Decreto nº 10.543, de 13 de novembro de 2020.

Documento assinado eletronicamente por **Sebastião Jose Nascimento de Padua**, **Professor(a)**, em 10/01/2025, às 15:17, conforme horário oficial de Brasília, com fundamento no art. 5º do Decreto nº 10.543, de 13 de novembro de 2020.

A autenticidade deste documento pode ser conferida no site https://sei.ufmg.br/sei/controlador_externo.php?acao=documento_conferir&id_orgao_acesso_externo=0, informando o código verificador **3760421** e o código CRC **A90160FE**.

Referência: Processo nº 23072.269165/2024-31 SEI nº 3760421

Acknowledgements

I want to express my gratitude for the years of financial support I have received through the doctoral grant: Bolsa CAPES-REUNI. These years of funding have been fundamental in my academic and professional development, allowing me to dedicate full time to my research work. I am profoundly grateful for this opportunity to the Postgraduate Program on Physics of the Universidade Federal de Minas Gerais - UFMG and the Instituto de Ciencias Exatas - ICEx. To the CNPq and Fapemig agencies for providing the necessary funds for the creation, implementation and maintenance of the Semiconductors Laboratory. To the professors of the Physics Postgraduate Program from whom I learned various aspects of advanced physics. I want to express my special gratitude to Professor Paulo Sérgio Soares Guimarães for his great teachings and enormous patience during my doctoral studies and research. To professors Boris Angelo Rodríguez and Herbert Vinck for the contributions made during my doctoral training. To Professor José Maria Villas-Bôas for his ideas and contributions to the completion of the thesis and scientific articles. To my friends, colleagues and lab mates specially to Gabriel Fagundes, Michel Silva, Mónica Bolivar, Luis Poveda, Mariana Poveda, P.E. Fabiano, Adriana Vargas, Eduar Valenzuela, Alix Bastidas, Thiago Graciano, Luisa Ramirez, Rafael Rojas, Juan Vasco, Thiago Silva, Barbara and Barbara, Juliana for the friendship offered and for their patience. To my wife, Edith Milena, for her patience and for tolerating my temperament, to my daughter Victoria for giving new strength to my life. To my sister Cathy and my nieces Angelhina and Estefania, for giving me their joy. To my parents Carmenza (R.I.P) and Luis Antonio (R.I.P), who from heaven, are surely witnessing all these achievements.

Resumo

A interação entre luz e matéria em sistemas quânticos abertos atraiu uma atenção significativa nas últimas décadas devido à sua importância no desenvolvimento de tecnologias quânticas emergentes, como a computação quântica e as comunicações ópticas. Nesse contexto, sistemas de microcavidades acoplados a pontos quânticos e nanostruturas têm sido objeto de extensos estudos teóricos e experimentais devido à sua capacidade de controlar e manipular fenômenos quânticos fundamentais. Este trabalho reúne três estudos de pesquisa que, embora abordem diferentes aspectos das interações luz-matéria, compartilham um interesse comum em explorar os efeitos do bombeio incoerente e dos processos de decoerência nas propriedades ópticas de sistemas quânticos abertos.

O primeiro estudo foca no efeito do bombeio incoerente de excitons sobre a retificação óptica de uma nanostrutura que interage com um campo óptico clássico monocromático. Usando uma equação mestra de Born-Markov na forma de Lindblad, a emissão espontânea, o desfasamento e o bombeio incoerente são incluídos na análise. Uma expressão analítica é derivada para descrever a retificação óptica em função da taxa de bombeio incoerente, mostrando como o sistema transita entre os regimes de bombeio fraco e forte.

O segundo trabalho examina o comportamento do espectro de fotoluminescência de um ponto quântico dentro de uma microcavidade semicondutora, sob a influência de um campo magnético externo. O sistema é modelado numericamente usando uma equação mestra na forma de Lindblad para capturar os efeitos da emissão espontânea, das perdas através dos espelhos da cavidade e do defasamento. Este trabalho revela a transição do regime de acoplamento forte para o regime da emissão desacoplada à medida que o campo magnético aumenta, com a linha σ_- no espectro desacoplando-se mais rapidamente.

O terceiro estudo investiga teoricamente os espectros de potência em um sistema de microcavidade-ponto quântico sob bombeio incoerente de fótons e excitons. Dois modelos diferentes são examinados, relacionando as taxas de perdas da cavidade e o bombeio, e são analisadas as transições entre os regimes de acoplamento forte e fraco em diferentes intensidades de bombeio. Apesar das diferenças entre os modelos, ambos preveem uma sequência de transições entre acoplamento fraco e forte à medida que o bombeio aumenta, um fenômeno que ainda não foi observado experimentalmente.

Embora esses três trabalhos abordem diferentes aspectos e sistemas quânticos, todos compartilham o objetivo comum de entender como o bombeio incoerente e os processos de decoerência afetam as propriedades ópticas e os regimes de acoplamento de sistemas quânticos abertos. Esses estudos não apenas fornecem novos *insights* teóricos, mas também

oferecem previsões que podem orientar futuros experimentos no campo da óptica quântica e das nanocavidades.

Palavras-chave: Interação luz-matéria, sistemas quânticos abertos, bombeio incoerente, decoerência, retificação óptica.

Abstract

The interaction between light and matter in open quantum systems has attracted significant attention in recent decades due to its importance in the development of emerging quantum technologies, such as quantum computing and optical communications. In this context, microcavity systems coupled to quantum dots and nanostructures have been the subject of extensive theoretical and experimental studies due to their ability to control and manipulate fundamental quantum phenomena. This work brings together three research studies that, while addressing different aspects of light-matter interactions, share a common interest in exploring the effects of incoherent pumping and decoherence processes on the optical properties of open quantum systems.

The first study focuses on the effect of incoherent exciton pumping on the optical rectification of a nanostructure interacting with a monochromatic classical optical field. Using a Born-Markov master equation in the Lindblad form, spontaneous emission, dephasing, and incoherent pumping are included in the analysis. An analytical expression is derived that describes optical rectification as a function of the incoherent pumping rate, showing how the system transitions between weak and strong coupling regimes.

The second work examines the behavior of the photoluminescence spectrum of a quantum dot within a semiconductor microcavity, under the influence of an external magnetic field. The system is numerically modeled using a Lindblad-form master equation to capture the effects of spontaneous emission, losses through cavity mirrors, and dephasing. This work reveals the transition from the strong coupling regime to uncoupled emission as the magnetic field increases, with the σ_- line in the spectrum decoupling more rapidly.

The third study investigates theoretically the power spectra in a microcavity-quantum dot system under incoherent pumping of photons and excitons. Two different models are examined, relating cavity loss rates and pumping; and transitions between strong and weak coupling regimes at different pumping intensities are analyzed. Despite differences between the models, both predict a sequence of transitions between weak and strong coupling as the pumping increases, a phenomenon that has yet to be observed experimentally.

Although these three works address different aspects and quantum systems, they all share the common goal of understanding how incoherent pumping and decoherence processes affect the optical properties and coupling regimes of open quantum systems. These studies not only provide new theoretical insights but also offer predictions that may guide future experiments in the field of quantum optics and nanocavities.

Keywords: Light-matter interaction, Open quantum systems, Incoherent pumping, Decoherence, Optical rectification.

Contents

1 Introduction

Due to its potential applications in the fields of computing [1], photonics [2], nanotechnology [3], and metrology [4], among others [5], the control of optical and electrical properties in semiconductor devices with nanometric dimensions has attracted great scientific and technological interest. The basis of this technology consists in preparing, controlling and taking advantage, efficiently, of the quantum states of structures composed of hundreds or thousands of atoms arranged in a special way. The main difficulty is to reduce the effects of decoherence produced by the interactions between thousands of atoms and impurities present in semiconductor materials.

At present, the quantum effects that have been achieved in semiconductor structures are comparable to the developments attained in systems of atoms. For example, the analog of the superposition of light-atom states developed experimentally by Haroche and his group [6,7] was achieved with cavity-quantum dot heterostructures developed by Reithmaier et al. [8] and others. This control was achieved through the development of atom by atom growth techniques such as molecular beam epitaxy (MBE) combined with nanolithographic processing techniques.

Similar to the atomic case, in semiconductor physics the principle of operation of the superposition of light-matter quantum states is based on the coupling of light quantum states obtained from light-confining structures with high quality factors such as micropillars, photonic crystals, nano-discs or nano-spheres, which make it possible to preserve light quantum states for a long time, and quantum states of matter obtained from structures such as quantum wires, quantum wells or quantum dots, which confine electric charge in one, two and three dimensions, respectively.

The physics behind these achievements is attributed to the ability to modify and control the electromagnetic density of states in the case of optical cavities, and the electronic density of states in the case of matter. Another possible way of modification of the structure of the electronic density of states is the inclusion of an external field, as a magnetic field for example. As in the atomic system, for example, for a quantum dot (QD) in the presence of an external magnetic field its spectral lines split; an effect known as Zeeman effect.

When the interaction between the quantum states of light and matter is sufficiently large, quantum states are obtained with combined characteristics of light and matter. This is the case of the exciton-polariton quasi-particle, which is a quantum effect resulting from the strong coupling of photons and excited states of matter (excitons) of a nanostructure. This type of particle can be evidenced in the luminescence spectrum of the material, in

which there is a separation of two lines in the emission spectrum of the material, an effect called Rabi splitting. This separation into two lines indicates that light and matter are strongly coupled and when this is not achieved it is considered that the states of light and matter are weakly coupled. In QDs, the Zeeman effect is useful to manage the tuning of the QDs levels with the cavity modes and to obtain control of the semiconductor light-matter coupling.

All of these developments form a new platform to study quantum effects in one single and relatively simple structure and also form the basis for possible new applications.

The works presented in this thesis are theoretical proposals that should be useful for the experimental researcher in the investigation of the coupling properties of cavity - quantum dot systems. To perform the corresponding calculations, many assumptions have to be done:

- Our motivation is semiconductor self-assembled quantum dots, which are obtained by the Stranski-Krastanov growing method. Such quantum dots can have different shapes (lens, pyramid, semi-spherical, ...). Since we are not interested in calculating the exact values of the energy levels of the quantum dots, we will not worry about their specific shape.
- The number of quantum dots in our system will be one or two, depending on our needs.
- We will consider only one exciton in each quantum dot.
- We will restrict our cavity to a semiconductor micropillar case.
- When the magnetic field is used, it will be considered constant and applied along the growth direction of the quantum dots.

This thesis is a compilation of previously published work by the author, in the area of coupling effects, incoherent pumping and influence of an external magnetic field in quantum dot-cavity systems. These references are:

- Portacio, A.A., Cano, L.E., Rasero, D.A. (2021). Optical rectification in self-assembled quantum dots: The role of incoherent pumping. Superlattices and Microstructures, 156, 106937.
- Cano, L.E., Guimaraes, P.S.S., Portacio, A. (2018). Efecto del campo magnético sobre el espectro de emisión para un sistema microcavidad-punto cuántico. Rev. Cubana Fis, 35, 115.

- L.E. Cano, J.M. Villas-Bôas, P.S.S. Guimarães (2024). Weak to strong coupling conditions for a microcavity-quantum dot system under incoherent pumping. Physica B 591, 416282.

Next, some important concepts necessary to understand each of the previous references will be presented.

The first concept is the Jaynes-Cummings model. This model is a simple quantum mechanical model that includes the light-matter interaction of a single cavity mode with a two-level system. The principal characteristic of this model is the oscillating behavior of the populations of light and matter states due to the coupling. These oscillations, known as Rabi oscillations, are characteristic of quantum mechanical systems.

The second concept is Lindblad dynamics. The realistic necessity to put a quantum system in an environment has led to the development of the theory of open quantum systems. In these developments, the system and the environment are considered to be coupled in a way that the system is affected by the environment, but the environment is not significantly affected by the system. Additionally, the system does not have a memory term. With these approximations, the quantum evolution of the system's state is represented as a set of differential equations and operators that allow us to study the dynamics of the system.

The third concept is the Power Spectra observable. The light emission spectrum is a characteristic of quantum systems that reflects many aspects of the internal behavior of the system, such as energy levels and coupling strengths. Quantum mechanically, the light emission spectrum is defined as the Fourier transform of the mean value of the two-times correlation of the light operator. This quantity is directly related to the luminescence spectra measured in experimental works.

The last concept to understand principally, specially in the context of the first work described in this thesis, is the optical rectification term. When a material is subjected to a light beam, it can become polarized as a result of the light's influence. The level of this polarization is directly correlated to the intensity of the electric field acting on the material. The linear component of this relationship is referred to as linear optical susceptibility, while the second-order component is known as optical rectification.

These concepts are explained in more detail in the next chapter and its associated references.

2 Theoretical Frame

2.1 Simple quantum model for light-matter interaction

2.1.1 Jaynes-Cummings model

The Jaynes-Cummings model [9, 10] describes the interaction of a two level system, indicated by the excited $|X\rangle$ and the ground $|G\rangle$ states, with a single mode of the radiation field represented as

$$\overrightarrow{E} = \hat{e}\left(\frac{\hbar\omega}{\epsilon_0 V}\right)^{1/2}(\hat{a}^\dagger + \hat{a})sin(kz), \tag{2.1}$$

where $\hat{e}$ is a polarization vector, $\hat{a}\,(\hat{a}^\dagger)$ is the light annihilation (creation) operator, and k is the wave vector in the z-direction. The constants $\hbar$, ω, ϵ_0 and V are, respectively, Planck's constant divided by 2π, the angular frequency, the vacuum permittivity and the volume of the system.

The total Hamiltonian can be written as

$$\hat{H} = H_{\text{T.L.}} + H_{\text{field}} + H_{\text{Int.}}, \tag{2.2}$$

where $H_{\text{T.L.}}$ is the two level Hamiltonian, H_{field} represents the single electromagnetic mode, and $H_{\text{Int.}}$ is used to describe the interaction between the two level system (TL) and the single electromagnetic mode. If we consider the zero of energy as the halfway point between the levels $|X\rangle$ and $|G\rangle$, which have a difference of energy $E_X - E_G = \hbar\omega_0$, and with the help of the operator $\hat{\sigma}_z = |X\rangle\langle X| - |G\rangle\langle G|$, $H_{\text{T.L.}}$ can be written as $H_{\text{T.L.}} = \frac{1}{2}\hbar\omega_0\hat{\sigma}_z$. The Hamiltonian for the electromagnetic single mode field is $H_{\text{field}} = \hbar\omega\,\hat{a}^\dagger\hat{a}$, where the zero-photons energy $\frac{1}{2}\hbar\omega$ was neglected. The interaction Hamiltonian in the dipole approximation is the dipole operator $\hat{d} = d(\hat{\sigma}_+ + \hat{\sigma}_-)$ multiplied by the operator $\hat{E}$ (equation 2.1). Here, $d = \langle X|\hat{d}|G\rangle$ is the dipole element of the operator $\hat{d}$. We obtain $H_{\text{Int.}} = \hbar g(\hat{\sigma}_+ + \hat{\sigma}_-)(\hat{a}^\dagger + \hat{a})$, where $\hat{\sigma}_+ = |X\rangle\langle G|$, $\hat{\sigma}_- = |G\rangle\langle X|$ and $g = \frac{d}{\hbar}\left(\frac{\hbar\omega}{\epsilon_0 V}\right)^{1/2} sin(kz)$. With these definitions the Hamiltonian takes the form

$$\hat{H} = \frac{1}{2}\hbar\omega_0\hat{\sigma}_z + \hbar\omega\,\hat{a}^\dagger\hat{a} + \hbar g(\hat{\sigma}_+ + \hat{\sigma}_-)(\hat{a}^\dagger + \hat{a}). \tag{2.3}$$

2.1.1.1 The rotating wave approximation and the Jaynes-Cummings Hamiltonian

Another approximation used in this model is the rotating wave approximation (RWA). This approximation consists in maintaining in the interaction Hamiltonian only the transitions that couple the excitation of matter with a deexcitation of the electromagnetic field and vice versa. This approximation brings the Jaynes-Cummings Hamiltonian to the

form

$$\hat{H} = \frac{1}{2}\hbar\omega_0\hat{\sigma}_z + \hbar\omega\hat{a}^\dagger\hat{a} + \hbar g(\hat{\sigma}_+\hat{a} + \hat{\sigma}_-\hat{a}^\dagger). \tag{2.4}$$

Because the Hamiltonian only takes account of single photon transitions with the corresponding excitation of matter, it is possible to write the Hamiltonian in a block form. In the base of states for a number n of photons, the possible transitions are between the states known as bare states, $|X\rangle|n\rangle \leftrightarrow |G\rangle|n+1\rangle$. The n-block of the Hamiltonian has the form

$$H_{(n)} \doteq \begin{pmatrix} \frac{1}{2}\hbar\omega_0 + n\hbar\omega & \hbar g\sqrt{n+1} \\ \hbar g\sqrt{n+1} & -\frac{1}{2}\hbar\omega_0 + (n+1)\hbar\omega \end{pmatrix}, \tag{2.5}$$

with eigen-energies written in terms of a detuning parameter $\Delta = \omega - \omega_0$,

$$E_{+/-} = \frac{\hbar}{2}\left((1+2n)(\Delta+\omega_0) \pm \sqrt{\Delta^2 + 4(1+n)g^2}\right) \tag{2.6}$$

and eigenvectors,

$$|n,+\rangle = \cos\left(\frac{\theta}{2}\right)|X\rangle|n\rangle + \sin\left(\frac{\theta}{2}\right)|G\rangle|n-1\rangle, \tag{2.7}$$

$$|n,-\rangle = -\sin\left(\frac{\theta}{2}\right)|X\rangle|n\rangle + \cos\left(\frac{\theta}{2}\right)|G\rangle|n-1\rangle, \tag{2.8}$$

typically known as dressed states. Here, $\tan\left(\frac{\theta}{2}\right) = \frac{\Delta+\Omega(\Delta)}{\Omega(0)}$, $\Omega(\Delta) = [\Delta^2 + 4g^2(n+1)]^{1/2}$ and $\Omega(0) = 2g(n+1)^{1/2}$.

The most important contribution that the Jaynes-Cummings model brings is the possibility to study light-matter transitions in a complete quantum mechanics formalism. A physical consequence of this treatment is the prediction of the collapses and revivals of the atomic populations for a special case of the electromagnetic field (a coherent state).

2.2 Simple models for quantum dots, cavities and light-matter interac.

2.2.1 Semiconductor quantum dots

One of the most prominent advantage of the semiconductor quantum dots is the ability to confine charge in a very narrow region of the space, quantizing the electron (and hole) energy levels. This discrete behavior gives the possibility of relaxation of energy in a discrete manner, giving rise to an emission spectrum that is similar to that of atoms. For that reason the semiconductor quantum dots are usually called artificial atoms.

Semiconductor quantum dots (QDs) growth techniques have been developed mainly in two branches: colloidal solutions, that use chemical reactions to obtain the QD [11], and epitaxial growth [12], where the materials are deposited on substrates, layer by layer,

in a controlled way. Here, we only explain the technique called molecular beam epitaxy in the Stranski-Krastanov regime [13]. This technique consists in the growth of thin films of two or more semiconductor materials of different lattice constants, which cause strain forces that generates spontaneous formation of "islands", processes that relaxes the strain forces. Those "islands" are our self-assembled quantum dots.

The complexity of the strain mechanism makes that the quantum dots can grow in different shapes, *i.e.,* they could adopt the form of pyramids, cylinders, semi-spheres, lenses, depending of the growth parameters.

Some control of the size and shape of the quantum dot is possible, by adjusting the growth parameters. Unfortunately, normally there is no control of the position where the quantum dots will grow. Some developments in this aspect come from the growth on substrates with a well determined defect pattern. In this kind of sample the self-assembled quantum dots can be grown in predictable positions [14, 15]. The method of achieving the growth of quantum dots in specific positions is still a matter of intensive study.

In the theoretical aspect, some different shapes of the confining potential are adopted, such as spheres, cylinders and pyramids, allowing the possibility to model discrete energy levels of the carriers inside the quantum dot. Another possibility supported by the experimental evidence [13] is that it is possible to consider most self-assembled quantum dots as a harmonic (parabolic) potential of confinement.

2.2.2 The exciton

In a semiconductor material, the exciton is a kind of particle formed when an electron in the conduction band is bounded with a hole in the valence band by the Coulomb force. The bound energy of this particle is typically of the order of a few meV and its characteristic lifetime is some nanoseconds. The recombination of the pair can be in a radiative process emitting light or in non-radiative processes heating the system due to interactions with the lattice. Figure 2.1 shows a schematic representation of the interaction between one photon and a bounded electron-hole pair, the excition.

2.2.3 Photonic Cavities

A photonic crystal is a system that combines two or more dielectric materials in a periodic arrangement leading to the formation of a photonic band structure [16]. The periodic variation of the refraction index can result in the appearance of bands of allowed and bands of forbidden frequencies; the latter are usually called photonic band gaps. The most important property of a photonic crystal is the property to enhance or forbid the flux of light of some wavelengths in the direction of periodicity of the system. Also, the presence of the band gap can be used to control the flux of light.

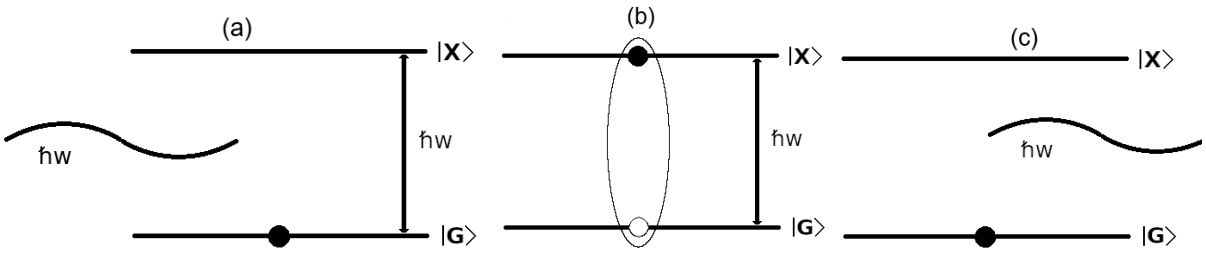

Figure 2.1 – Schematic representation of a quantum dot within a two-level approximation, where $|G\rangle$ denotes the ground state and $|X\rangle$ the excited state. (a) The quantum dot system in the ground state $|G\rangle$ and an incident light of frequency ω. (b) Creation of an exciton (electron-hole pair) due to light absorption. (c) Photon emission during the annihilation of the exciton.

If some defects in the periodicity of the dielectric material are introduced, frequencies inside the band gap could now be allowed. These frequencies are localized near the region of the defects, thus confining the light with the formation of an optical cavity. Some typical configurations of these cavities are a pillar cavity [17], a L3 cavity [18], and others [19]. Specially, a pillar cavity is a one dimensional system in which light is trapped using the effect of confinement of light of a one dimensional photonic crystal (periodic variation of the refraction index in one dimension) and a lateral confinement of light using total internal reflection, with the critical angle for this confinement determined by the difference between the refractive indexes of the pillar material and of its surroundings.

2.2.4 Exciton-polariton

The exciton-polariton is a particle formed by the exciton strongly coupled with a photon, in such way that their behavior cannot be described as separable particles.

In this part of this work, we present a short historical presentation of the exciton-polariton concept. The exciton-polariton concept was first introduced by Hopfield [20] in 1958, in an intent to give a more complete view of the absorption process. This work formulates the optical properties of excitons in a quantum-electrodynamical treatment, developing an exciton-photon interaction Hamiltonian theory for the absorption process in an infinitely extended bulk material. The next development in the area of polaritons took nearly four decades: the control of the polariton behavior. The work of Weisbuch et al. [21] was the study that showed for the first time the mode splitting of quantum-well excitons, using the spectral response of a semiconductor microcavity and quantum wells in the strong-coupling regime. This work explicitly shows the need to take account of the dimensionality effects in quantum confined systems in order to obtain a control of the optical properties of these systems. With these ideas in mind, Houdre et al. [22] showed the experimental behavior of the intensity of the photoluminescence spectrum, reporting

that the strong coupling regime saturates under high excitation power. This latter work uses the properties of a quantum-well exciton inserted in semiconductor microcavities. The special interest with this study is that it contributes to the characterization of the two regimens of coupling, the strong-coupling and the weak-coupling, finding that the strong-coupling regime has a saturation point caused by the non-resonant electron-hole pairs. With the knowledge obtained about photoluminescence measurements, Tartakovski et al. [23] studied the behavior of the dispersion of polaritons in semiconductor microcavities with two-dimensional light confinement. They found that the strong exciton-photon coupling can be suppressed when the exciton densities are increased. The same idea was explored in other geometrical microcavities configurations [19]. Photoluminescence measurements were reported by Bloch et al. [24] in pillar microcavities and GaAs quantum-wells. Gutbrod et al. [25] studied the photoluminescence of photons and excitons in photonic dots. In this work it was reported that the photon energies are a function of the dot size and shape and the changes in the exciton-photon coupling due to the confinement were studied. After all of these experimental works, it was possible to formulate for the first time the idea of polariton lasing. Cao et al. [26] were the ones responsible for this discovery. They presented experimental data for the microcavity polariton system at high density, interpreting the experimental data obtained as the existence of a region where the lasing process was possible. Another interesting fact in the polariton concept was developed with the study of Deng et al. [27]. That work shows the existence of a phase transition from a classical thermally mixed state to a quantum-mechanical pure state of exciton polaritons in a GaAs multiple quantum-well microcavity, confirming the condensation of microcavity exciton-polaritons. For quantum dots immersed in microcavities the studies are still in progress after the pioneering work of J. Gao et al. [28].

2.3 Master equation: for a more realistic dynamics

The models described before do not take account of the interaction with the environment. It is possible to include characteristic environments to these models through an approach called the master equation. This approach describes the time evolution of the process, and includes the non-unitary effects that destroy the quantum behavior of a system.

The Lindblad form is a formulation of the master equations written as a set of differential equations for the density matrix operator, $\hat{\rho}$, of the system, describing the time evolution of the probabilities of the occupation of each state. The master equation in the Lindblad form [1] has two important approximations: the **Born approximation**, where the environment is considered to be huge relative to the system, leaving the states of the environment and the system separable; and the **Markov approximation**, where no memory effect of the environment on the system is taken into account.

The master equation in the Lindblad form is

$$\frac{d\hat{\rho}}{dt} = -\frac{i}{\hbar}[\hat{H}, \hat{\rho}] + \sum_j \left(2L_j\hat{\rho}L_j^\dagger - \{L_j^\dagger L_j, \hat{\rho}\}\right) \tag{2.9}$$

where the L_j are the non-unitary operators that model the coupling of the system for the different environments and $\{\hat{A}, \hat{B}\} = \hat{A}\hat{B} + \hat{B}\hat{A}$ is the anti-commutation operation for arbitrary operators $\hat{A}$ and $\hat{B}$. It is better to explain all of these with a specific example. Here, we will follow the work of Perea et al. [29], where the system is a quantum dot in a microcavity, and the interactions with environments that are considered are the coupling with the vacuum state producing spontaneous emission processes, loss of photons from the system for a non-perfect cavity, and incoherent pumping of excitons, which is a form of populating the system with particles. All of this leads to the master equation,

$$\begin{aligned}\frac{d\hat{\rho}}{dt} = &-\frac{i}{\hbar}[\hat{H}, \hat{\rho}] + \frac{\Gamma_x}{2}\left(2\hat{\sigma}\hat{\rho}\hat{\sigma}^\dagger - \{\hat{\sigma}^\dagger\hat{\sigma}, \hat{\rho}\}\right) + \frac{\Gamma_c}{2}\left(2\hat{a}\hat{\rho}\hat{a}^\dagger - \{\hat{a}^\dagger\hat{a}, \hat{\rho}\}\right) \\ &+ \frac{P_c}{2}\left(2\hat{a}^\dagger\hat{\rho}\hat{a} - \{\hat{a}\hat{a}^\dagger, \hat{\rho}\}\right) + \frac{P_x}{2}\left(2\hat{\sigma}^\dagger\hat{\rho}\hat{\sigma} - \{\hat{\sigma}\hat{\sigma}^\dagger, \hat{\rho}\}\right)\end{aligned} \tag{2.10}$$

where Γ_x represents the spontaneous emission rate, Γ_c is the loss of photons from the system, P_c is the rate of continuous incoherent pumping of photons and P_x is the rate of continuous incoherent pumping of excitons. Note the difference in the order of the operators for the pumping term with respect to the operators for the spontaneous emission and loss of photons. The pumping terms in the Lindblad equation describe any kind of particles that is incoming to the system, *i.e.,* incoming excitons or photons, and the other terms describe outgoing particles.

When the Lindblad dynamics describe the interaction of the quantum dot with the microcavity, the natural solution typically leads to an equilibrium or steady-state solution for the density matrix ρ. Under certain conditions where the system is in resonance with the cavity mode and there is a weak coupling between the emitter and the cavity, the system reaches a steady state characterized by an enhanced emission rate, that is the so-called Purcell effect. On the other side, when the coupling emitter-cavity is strong enough, we have the formation of a quasi-particle, the exciton-polariton.

2.4 Theory of the photoluminescence spectra using the Green method

The photoluminescence spectra $s(\omega)$ is defined as the light emitted by a system observed in its frequencies components, i.e., it is the field intensity for a given frequency. The photoluminescence spectra is usually calculated by the Fourier transform of the electric

field intensity and this intensity is related with the mean number of photons emitted by a system in a determined angular frequency $\langle \hat{a}^\dagger(\omega)\hat{a}(\omega)\rangle$.

Here, we calculate the spectra using the relation that exists between $\langle \hat{a}^\dagger(\omega)\hat{a}(\omega)\rangle$ and the Fourier transform of the average of the two-times first order correlation function $K(t) \equiv \langle \hat{a}^\dagger(t)\hat{a}(0)\rangle$ [30]. This relation is written as

$$s(\omega) = 2Re \int_0^\infty K(t) e^{-i\omega t} dt. \tag{2.11}$$

The $K(t)$ operator is calculated using the density matrix theory, i.e., for an arbitrary operator $\hat{A}$ the mean value is defined as $\langle \hat{A} \rangle = Tr[\hat{A}\rho]$, where Tr represents the trace of the product of the density matrix $\hat{\rho}$ and the operator $\hat{A}$. If we have a composed system, the density matrix describes two or more subsystems. For the mean values of a given operator, we used the partial trace operator to calculate the density matrix operator that describes the subsystem and used it to calculate the mean value. In the case that the density operator represents matter states and light modes, the mean value for the two-times operator $\langle \hat{a}^\dagger(t)\hat{a}(0)\rangle$ has to be calculated using the relation

$$K(t) = Tr_{\rho_{mat.}} \left[\sum_{n,m,l=0}^{\infty} \sqrt{l(m+1)} U_{l-1,m}(t) \langle m+1| \hat{\rho} |n\rangle U^\dagger_{n,l}(t) \right], \tag{2.12}$$

where $U_{l-1,m}(t) = \langle l-1| \hat{U}(t) |m\rangle$, $U^\dagger_{n,l}(t) = \langle n| \hat{U}^\dagger(t) |l\rangle$ and the partial trace Tr_{Light} operation was made over light state $|n\rangle$. The symbol $Tr_{\rho_{mat.}}$ represents trace over matter states.

With the assumption that at the steady state the density operator can be written in a separable way from matter and light, the density matrix at the steady state is $\hat{\rho}^{(SS)} = \hat{\rho}^{(SS)}_{mat.} \otimes \hat{\rho}^{(SS)}_{Light}$, where the symbol (SS) represents steady state and $K(t)$ can be written as

$$\begin{aligned} K(t) &= Tr^{(SS)}_{\rho_{mat.}} \left[\sum_{n,m,l=0}^{\infty} \sqrt{l(m+1)} U_{l-1,m}(t) \langle m+1| \hat{\rho}_{mat.} \otimes \hat{\rho}_{Light} |n\rangle U^\dagger_{n,l}(t) \right] \\ &= \sum_{n,m,l=0}^{\infty} Tr_{\rho_{mat.}} \left[U_{l-1,m}(t) \hat{\rho}_{mat.} U^\dagger_{n,l}(t) \right] \sqrt{l(m+1)} \langle m+1| \hat{\rho}_{Light} |n\rangle \\ &= \sum_{n,m,l=0}^{\infty} G_{n,m,l}(t) \sqrt{l(m+1)} \langle m+1| \hat{\rho}_{Light} |n\rangle , \end{aligned} \tag{2.13}$$

where $G_{n,m,l}(t) = Tr_{\rho_{mat.}} \left[U_{l-1,m}(t) \hat{\rho}_{mat.} U^\dagger_{n,l}(t) \right]$ is usually called the Green function of the system.

An initial condition for the Green function $G_{n,m,l}(0)$ is obtained applying the definition of the $\hat{U}$ operators for the time $t = 0$, $U_{l-1,m}(0) = \langle l-1| |m\rangle = \delta_{l-1,m}$, and

$U^{\dagger}_{n,l}(0) = \langle n|\,|l\rangle = \delta_{n,l}$, leading to the initial condition as

$$G_{n,m,l}(0) = \delta_{l-1,m}\delta_{n,l}, \tag{2.14}$$

where we use the fact that $Tr_{\rho_{mat.}}\left[\hat{\rho}_{mat.}\right] = 1$.

With the assumption that the density matrix for light is diagonal,

$$\begin{aligned}\langle m+1|\,\hat{\rho}^{(SS)}_{Light}\,|n\rangle &= \delta_{m+1,n}\,\langle n|\,\hat{\rho}^{(SS)}_{Light}\,|n\rangle \\ &= \delta_{m+1,n}P_n,\end{aligned} \tag{2.15}$$

where $P_n = \langle n|\,\hat{\rho}^{(SS)}_{Light}\,|n\rangle$, the function $K(t)$ can be written as

$$\begin{aligned}K(t) &= \sum_{n,m,l=0}^{\infty} Tr_{\rho_{mat.}}\left[U_{l-1,m}(t)\hat{\rho}^{(SS)}_{mat.}U^{\dagger}_{n,l}(t)\right]\sqrt{l(m+1)}\,\langle m+1|\,\hat{\rho}^{(SS)}_{Light}\,|n\rangle \\ &= \sum_{m,l'=0}^{\infty} G_{l',m}(t)\sqrt{(l'+1)(m+1)}P_{m+1},\end{aligned} \tag{2.16}$$

where the Green function is $G_{l',m}(t) = Tr_{\rho_{mat.}}\left[U_{l',m}(t)\hat{\rho}^{(SS)}_{mat.}U^{\dagger}_{m+1,l'+1}(t)\right]$, and the variable replacement $l' = l-1$ was used.

The initial condition for this Green function is

$$\begin{aligned}G_{l',m}(t=0) &= Tr_{\rho_{mat.}}\left[U_{l',m}(0)\hat{\rho}^{(SS)}_{mat.}U^{\dagger}_{m+1,l'+1}(0)\right] \\ &= Tr_{\rho_{mat.}}\left[\langle l'|m\rangle\,\hat{\rho}^{(SS)}_{mat.}\,\langle m+1|l'+1\rangle\right] \\ &= \langle l'|m\rangle\,Tr_{\rho_{mat.}}\left[\hat{\rho}^{(SS)}_{mat.}\right] \\ &= \langle l'|m\rangle\,.\end{aligned} \tag{2.17}$$

The Green function $G_{l',m}$ is interpreted as the off-diagonal element for light modes

$$G_{l',m} = \langle l|\,G^{(m)}\,|l+1\rangle \tag{2.18}$$

$$\begin{aligned}G_{l',m} &= Tr_{\rho_{mat.}}\left[\langle l'|\,U(t)\,|m\rangle\,\hat{\rho}^{(SS)}_{mat.}\,\langle m+1|\,U^{\dagger}(t)\,|l'+1\rangle\right] \\ &= \langle l'|\,\hat{G}^{(m)}_{l'}(t)\,|l'+1\rangle\,,\end{aligned} \tag{2.19}$$

where $\hat{G}^{(m)}_{l'}(t) = Tr_{\rho_{mat.}}\left[U(t)(|m\rangle\,\langle m+1|)\hat{\rho}^{(SS)}_{mat.}U^{\dagger}(t)\right]$ is the Green operator. To describe the time dependence of the Green function, it is useful to consider that the operator $\hat{G}^{(m)}_{l'}(t)$ must satisfy the same kind of equation that the light operator; because the light operator evolutes in the same way as the Green operator. That means that each Green function $G_{l',m} = \langle l'|\,\hat{G}^{(m)}\,|l+1\rangle$ satisfies the same equation of motion $(\hat{\rho}_{Light})_{l',l'+1} = \langle l'|\hat{\rho}_{Light}|l'+1\rangle$. It allows us to write the dynamics of the Green function in the known form of the density matrix operator.

2.5 Polarization in Nonlinear Quantum Optical Systems

In nonlinear optics, the study of polarization plays a crucial role in understanding the interactions between light and matter. Its importance lies in its ability to capture the response of a medium to an incident electromagnetic field, providing insights into the optical properties of materials. In this kind of systems, the behavior of polarization can be described by the susceptibility function, which quantifies the relationship between the induced polarization and the applied electric field. The linear susceptibility represents how the polarization depends linearly on the electric field, offering insights into how materials respond to weak fields. In the linear approximation, the polarization is written as [31, 32]:

$$P(t) = \epsilon_0 \chi E(t), \tag{2.20}$$

where P represents polarization, ϵ_0 is the permittivity of free space, χ is the linear susceptibility, and $E(t)$ is the electric field.

In contrast, stronger fields introduce a nonlinear component to the polarization, where higher-order processes, such as quadratic and cubic susceptibilities, become significant [31]. In these cases, the polarization is expressed as:

$$P(t) = \epsilon_0 \left(\chi E(t) + \chi^{(2)} E^2(t) + \chi^{(3)} E^3(t) + \cdots \right), \tag{2.21}$$

where $\chi^{(2)}$ and $\chi^{(3)}$ are the second- and third-order susceptibilities, respectively. For this equation to hold, it is essential that the polarization at time t depends instantaneously on the intensity of the electric field, a condition valid only in lossless, non-dispersive media, and in the absence of photoionization.

It is possible to apply the mathematical methods for open quantum systems to calculate the nonlinear optical susceptibility under external incoherent pumping. This is done using the following theoretical framework [33].

Use the Lindblad Master Equation to model the dynamics of open quantum systems, incorporating both the coherent evolution of the system and the dissipative effects due to spontaneous emission, incoherent pumping, dephasing or other incoherent process.

$$\frac{\partial \hat{\rho}}{\partial t} = \frac{1}{i\hbar} \left[\hat{H}_0 + \hat{V}(t), \hat{\rho} \right] + L[\rho], \tag{2.22}$$

where the Hamiltonian part describes the matter system (e.g., a quantum dot and its associated exciton) modeled as a two-level system, with the ground state $|g\rangle$ and excited state $|e\rangle$. Their interaction with monochromatic light is represented by $V(t) = -\overrightarrow{M} \cdot \overrightarrow{E}(t)$, where the term $\overrightarrow{M}$ denotes the dipole moment operator $\hat{M} = q\hat{x}$, with q being the particle charge and $\hat{x}$ the position operator. The dissipative Lindblad terms $L[\rho]$ are included to account for spontaneous emission, decoherence, and incoherent exciton pumping.

The solution to the density operator is proposed through a perturbative expansion, applied to solve the master equation by expanding the density operator and the electric field in powers of a parameter λ, enabling the calculation of the density matrix for different orders. The density matrix is expressed as:

$$\rho = \sum_{n=0}^{\infty} \lambda^n \rho^{(n)}, \tag{2.23}$$

where λ represents the order of perturbation, and the electric field is introduced in the expansion as:

$$E(t) \to \lambda E(t). \tag{2.24}$$

The expansion allows solving the master equation order by order, obtaining the density matrix for each expansion, which in turn leads to the polarization vector and the corresponding susceptibilities. The differential equations derived from the master equation are solved under the assumption of steady-state conditions, $t \to \infty$.

For each order, the value of the polarization operator is calculated as the expectation value of the dipole moment per unit volume V:

$$P = \frac{1}{V}\mathrm{Tr}[\rho \hat{M}]. \tag{2.25}$$

Finally, the linear and nonlinear polarization terms in the frequency domain are computed and compared with the classical polarization terms. This comparison provides the linear and nonlinear susceptibilities in the context of open quantum systems [33].

The procedure outlined here is applied in the chapter titled "Optical Rectification in Self-Assembled Quantum Dots: The Role of Incoherent Pumping." for the case of spontaneous emission and incohenrent pumping of excitons.

3 Optical rectification in self-assembled quantum dots: The role of incoherent pumping

The effect of the incoherent pumping of excitons on the optical rectification of a nanostructure that interacts with a monochromatic classical optical field is studied theoretically, by solving a Born-Markov master equation in the Lindblad form that includes the processes of spontaneous emission, dephasing, and incoherent pumping of excitons between two levels of the nano– structured quantum system. In addition, the quantum vacuum of the electromagnetic field that affects the nanostructure was considered as an environment for the system. An analytical expression for the optical rectification was found in terms of the incoherent pumping rate of excitons P in which a weak pumping regime and a strong pumping regime are evidenced.[1]

3.1 Introduction

Low dimensional semiconductor structures (LDSS) has been a branch in semiconductor physics of rapid development [34, 35]. This field has great importance due to its possible applications in areas such as quantum optics, nano-photonics [36], quantum information [37, 38], optoelectronics [39], quantum metrology [40] and quantum computation [41]. Inherently, its development was due to the advance in semiconductor growth techniques, which allowed the confinement of charge carriers in one, two, or three dimensions, producing quantum wells, quantum wires, and quantum dots (QD) structures, respectively. All of these structures led to the development of better infrared detectors [42], image sensors [43], laser diodes [44], and many other emerging technologies [45]. One of the main aims in the development of LDSS technology is to achieve a theoretical understanding and experimental control on the linear and non-linear optical response of LDSS [46]. Recently, in the theoretical side, the research was directed to the understanding and the exploration of nonlinear optical properties and response of nanostructures such as quantum dots in the presence of external magnetic [47] and electric fields [48], and laser driving [48]. For this purpose, an alternative theoretical methodology was reported, which uses the theory of quantum open systems to analyze spontaneous emission and dephasing processes, and which reproduces the accepted solution of the Liouville-Von Neuman equation with included Lindblad terms [33]. Here, we propose a further development of this theory, which includes a new term on the Lindblad master equation that models incoherent pumping of excitons. In work reported here, this theory is applied to study the optical rectification

[1] Published at Superlattices and Microstructures 156 (2021) https://doi.org/10.1016/j.spmi.2021.106937

response of self-assembled semiconductor quantum dots. In section 3.2 the model of the system to be studied is formulated and the dynamics of the system is proposed, in section 3.3 the results and discussions are presented and in section 3.4 the conclusions are shown.

3.2 Theoretical background

To model the system, the Born-Markov master equation in the Lindblad form [49] is used

$$\frac{\partial \widehat{\rho}_s}{\partial t} = \frac{1}{i\hbar}[\widehat{H}, \widehat{\rho}] + \sum_{\nu=1}^{3} \frac{\lambda_\nu}{2}(2\widehat{L}_\nu \rho \widehat{L}_\nu^\dagger - \widehat{L}_\nu^\dagger \widehat{L}_\nu \widehat{\rho} - \widehat{\rho}\widehat{L}_\nu^\dagger \widehat{L}_\nu) \tag{3.1}$$

where $\widehat{\rho}_s$ is the density matrix of the system, $\widehat{H}$ the Hamiltonian operator, $\widehat{L}$ are the Lindblad operators with λ as the coefficient rate. Spontaneous emission is defined as $\widehat{L}_1 = \widehat{\sigma}$ with rate $\lambda_1 = \gamma$, dephasing as $\widehat{L}_2 = \widehat{\sigma}_z$ with $\lambda_2 = \gamma_\varphi$ and the continuous and incoherent exciton pumping term $\widehat{L}_3 = \widehat{\sigma}^\dagger$, associated with a reservoir of quantum dots, at a pumping rate $\lambda_3 = P$ [50, 51]. Here the operators $\widehat{\sigma} = |g\rangle\langle e|$, $\widehat{\sigma}_z = |e\rangle\langle e| - |g\rangle\langle g|$ are operators in the frame of the theory for two-level systems for ground and excited states $\{|g\rangle, |e\rangle\}$, respectively.

To solve equation (3.1) for a Hamiltonian of a two levels system interacting with a monochromatic light $E(t)$ in the dipole approximation, we define the Hamiltonian as $\widehat{H} = \widehat{H}_0 + \widehat{V}(t)$, with $\widehat{V}(t) = -\widehat{M} \cdot E(t)$ and the dipolar moment operator $\widehat{M}$. The matrix elements of (3.1) are

$$\dot{\rho}_{eg} = -\left(i\omega_{eg} + \frac{\gamma}{2} + \frac{P}{2} + \gamma_\varphi\right)\rho_{eg} - \frac{1}{i\hbar}\left[\widehat{M}E(t), \widehat{\rho}\right]_{eg}, \tag{3.2}$$

$$\dot{\rho}_{ee} = -\gamma\rho_{ee} + P\rho_{gg} - \frac{1}{i\hbar}\left[\widehat{M}E(t), \widehat{\rho}\right]_{ee}, \tag{3.3}$$

$$\dot{\rho}_{gg} = \gamma\rho_{ee} - P\rho_{gg} - \frac{1}{i\hbar}\left[\widehat{M}E(t), \widehat{\rho}\right]_{gg}, \tag{3.4}$$

where ee, gg, eg are indexes that represent the corresponding matrix element.

To solve equations (3.2)–(3.4), a perturbation method is used, where the density matrix is expanded as $\widehat{\rho} = \sum_{n=0} \lambda^n \widehat{\rho}^{(n)}$ and $E(t) = \lambda E(t)$. We obtained a set of iterated equations. Specifically, the set of equations for zero-order are

$$\dot{\rho}_{eg}^{(0)} = -\left(i\omega_{eg} + \frac{\gamma}{2} + \frac{P}{2} + \gamma_\varphi\right)\rho_{eg}^{(0)}, \tag{3.5}$$

$$\dot{\rho}_{ee}^{(0)} = -\gamma\rho_{ee}^{(0)} + P\rho_{gg}^{(0)}, \tag{3.6}$$

$$\dot{\rho}_{gg}^{(0)} = \gamma\rho_{ee}^{(0)} - P\rho_{gg}^{(0)}, \tag{3.7}$$

and for the n-order are

$$\dot{\rho}_{eg}^{(n)} = -\left(i\omega_{eg} + \frac{\gamma}{2} + \frac{P}{2} + \gamma_{\varphi}\right)\rho_{eg}^{(n)} - \frac{1}{i\hbar}\left[\widehat{M}E(t), \widehat{\rho}^{(n-1)}\right]_{eg}, \tag{3.8}$$

$$\dot{\rho}_{ee}^{(n)} = -\gamma\rho_{ee}^{(n)} + P\rho_{gg}^{(n)} - \frac{1}{i\hbar}\left[\widehat{M}E(t), \widehat{\rho}^{(n-1)}\right]_{ee}, \tag{3.9}$$

$$\dot{\rho}_{gg}^{(n)} = \gamma\rho_{ee}^{(n)} - P\rho_{gg}^{(n)} - \frac{1}{i\hbar}\left[\widehat{M}E(t), \widehat{\rho}^{(n-1)}\right]_{gg}. \tag{3.10}$$

To achieve our goal to describe the effects of the incoherent pumping on the optical rectification, in the thermodynamic limit, the condition ($t \to \infty$) must be included to solve the iterated set of equations (3.5)–(3.10) and to study the optical response it is necessary to solve the expansion until second-order. For the zero-order solution

$$\rho_{eg}^{(0)}(t) \to \rho_{eg}^{(0)} = 0, \tag{3.11}$$

$$\rho_{ee}^{(0)}(t) \to \rho_{ee}^{(0)} = \frac{P}{\gamma + P}, \tag{3.12}$$

$$\rho_{gg}^{(0)}(t) \to \rho_{gg}^{(0)} = \frac{\gamma}{\gamma + P}, \tag{3.13}$$

while to first-order the solution is

$$\dot{\rho}_{eg}^{(1)} = -\left(i\omega_{eg} + \frac{\gamma}{2} + \frac{P}{2} + \gamma_{\varphi}\right)\rho_{eg}^{(1)} - \frac{E(t)M_{eg}(\rho_{gg}^{(0)} - \rho_{ee}^{(0)})}{i\hbar}, \tag{3.14}$$

$$\dot{\rho}_{ee}^{(1)} = -\gamma\rho_{ee}^{(1)} + P\rho_{gg}^{(1)}, \tag{3.15}$$

$$\dot{\rho}_{gg}^{(1)} = \gamma\rho_{ee}^{(1)} - P\rho_{gg}^{(1)}, \tag{3.16}$$

and for the second-order, the solution is

$$\dot{\rho}_{eg}^{(2)} = -\left(i\omega_{eg} + \frac{\gamma}{2} + \frac{P}{2} + \gamma_{\varphi}\right)\rho_{eg}^{(2)} - \frac{E(t)}{i\hbar}\rho_{eg}^{(1)}(M_{ee} - M_{gg}) \tag{3.17}$$

$$\dot{\rho}_{ee}^{(2)} = -\gamma\rho_{ee}^{(2)} + P\rho_{gg}^{(2)} - \frac{E(t)}{i\hbar}(M_{eg}\rho_{ge}^{(1)} - \rho_{eg}^{(1)}M_{ge}) \tag{3.18}$$

$$\dot{\rho}_{gg}^{(2)} = \gamma\rho_{ee}^{(2)} - P\rho_{gg}^{(2)} + \frac{E(t)}{i\hbar}(M_{eg}\rho_{ge}^{(1)} - \rho_{eg}^{(1)}M_{ge}) \tag{3.19}$$

Now, it is considered the change from time domain to the frequency domain as in Ref. [52]:

$$\rho_{nm}^{(2)}(t) = \widetilde{\rho}_{nm;0}^{(2)}(\omega) + \widetilde{\rho}_{nm;2\omega}^{(2)}(\omega)e^{-i2\omega t} + \widetilde{\rho}_{nm;2\omega}^{(2)}(-\omega)e^{i2\omega t}, \tag{3.20}$$

where $\widetilde{\rho}_{nm;0}^{(2)}(\omega)$ is the density matrix associated with the optical rectification and with the second order terms

$$\widetilde{\rho}_{eg;2\omega}^{(2)}(\omega) = \frac{(M_{ee} - M_{gg})\widetilde{\rho}_{eg;\omega}^{(1)}(\omega)\widetilde{E}(\omega)}{\hbar(\omega_{eg} - 2\omega) - i\hbar\left(\frac{\gamma}{2} + \frac{P}{2} + \gamma_{\varphi}\right)} \tag{3.21}$$

$$\widetilde{\rho}_{eg;0}^{(2)}(\omega) = \frac{(M_{ee} - M_{gg})\left(\widetilde{\rho}_{eg;\omega}^{(1)}(\omega)\widetilde{E}(-\omega) + \widetilde{\rho}_{eg;\omega}^{(1)}(-\omega)\widetilde{E}(\omega)\right)}{\hbar\omega_{eg} - i\hbar\left(\frac{\gamma}{2} + \frac{P}{2} + \gamma_{\varphi}\right)} \tag{3.22}$$

$$\widetilde{\rho}_{ee;2\omega}^{(2)}(\omega) = \frac{\gamma - 2i\omega}{\gamma + P - 2i\omega}\left(\frac{(M_{ge}\widetilde{\rho}_{eg;\omega}^{(1)}(\omega) - M_{eg}\widetilde{\rho}_{ge;\omega}^{(1)}(\omega))E(\omega)}{2\hbar\omega + i\hbar\gamma}\right) \tag{3.23}$$

$$\widetilde{\rho}_{gg;2\omega}^{(2)}(\omega) = \frac{\gamma - 2i\omega}{\gamma + P - 2i\omega}\left(\frac{(M_{ge}\widetilde{\rho}_{eg;\omega}^{(1)}(\omega) - M_{eg}\widetilde{\rho}_{ge;\omega}^{(1)}(\omega))E(\omega)}{2\hbar\omega + i\hbar\gamma}\right) \tag{3.24}$$

$$\widetilde{\rho}_{ee;0}^{(2)}(\omega) = \frac{\gamma}{(\gamma + P)}\left(\frac{(M_{ge}\widetilde{\rho}_{eg;\omega}^{(1)}(\omega) - M_{eg}\widetilde{\rho}_{ge;\omega}^{(1)}(\omega))E(-\omega)}{i\hbar\gamma} + \frac{(M_{ge}\widetilde{\rho}_{eg;\omega}^{(1)}(-\omega) - M_{eg}\widetilde{\rho}_{ge;\omega}^{(1)}(-\omega))E(\omega)}{i\hbar\gamma}\right) \tag{3.25}$$

$$\widetilde{\rho}_{gg;0}^{(2)}(\omega) = -\frac{\gamma}{(\gamma + P)}\left(\frac{(M_{ge}\widetilde{\rho}_{eg;\omega}^{(1)}(\omega) - M_{eg}\widetilde{\rho}_{ge;\omega}^{(1)}(\omega))E(-\omega)}{i\hbar\gamma} + \frac{(M_{ge}\widetilde{\rho}_{eg;\omega}^{(1)}(-\omega) - M_{eg}\widetilde{\rho}_{ge;\omega}^{(1)}(-\omega))E(\omega)}{i\hbar\gamma}\right) \tag{3.26}$$

The second order optical susceptibility is defined as

$$\begin{aligned} P^{(2)}(t) &= \frac{1}{V}Tr(\widehat{\rho}^{(2)}(t)\widehat{M}) \\ &= 2\epsilon_0\chi^{(2)}(\omega)\widetilde{E}(\omega)\widetilde{E}(-\omega) + \epsilon_0\chi_{2\omega}^{(2)}(\omega)\widetilde{E}^2(\omega)e^{-i2\omega t} + \epsilon_0\chi_{2\omega}^{(2)}(-\omega)\widetilde{E}^2(-\omega)e^{i2\omega t}, \end{aligned} \tag{3.27}$$

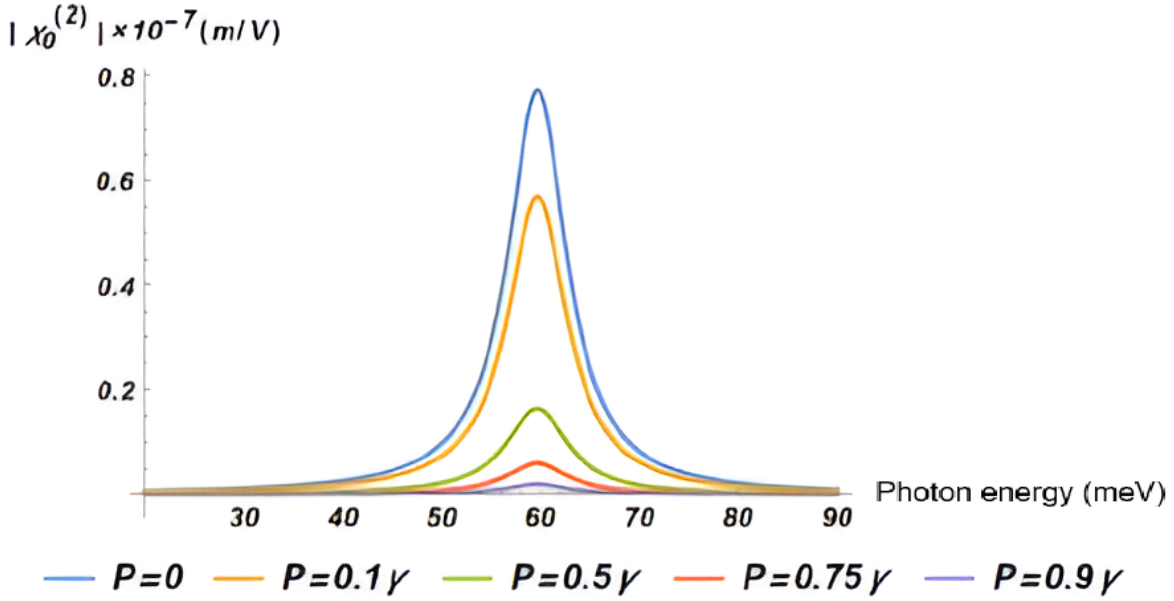

Figure 3.1 – The optical rectification coefficient (OR) as a function of the incident photon energy $\hbar\omega$ for five different values of incoherent pumping in the weak pumping regime (i.e., P $<$ γ), for a cylindrical QD with height L = 10 nm and radius R = 8 nm.

where V represents the volume of the system.

From equation (3.28), with the proper replacements (3.11)-(3.26) and without the anti-resonant term, we obtain the optical rectification equation

$$\chi_0^{(2)}(\omega) = \frac{(M_{ee}-M_{gg})(\rho_{gg}^{(0)}-\rho_{ee}^{(0)})}{2V\epsilon_0} \left(\left(\frac{\gamma}{(\gamma+P)}\frac{M_{ge}}{i\hbar\gamma}+\frac{M_{ge}}{\hbar\omega_{eg}-i\hbar\left(\frac{\gamma}{2}+\frac{P}{2}+\gamma_\varphi\right)}\right)\left(\frac{M_{eg}}{\hbar\omega_{eg}-i\hbar\left(\frac{\gamma}{2}+\frac{P}{2}+\gamma_\varphi\right)-\hbar\omega}\right) +\left(\frac{M_{eg}}{\hbar\omega_{eg}+i\hbar\left(\frac{\gamma}{2}+\frac{P}{2}+\gamma_\varphi\right)}-\frac{\gamma}{(\gamma+P)}\frac{M_{eg}}{i\hbar\gamma}\right)\left(\frac{M_{ge}}{\hbar\omega_{eg}+i\hbar\left(\frac{\gamma}{2}+\frac{P}{2}+\gamma_\varphi\right)-\hbar\omega}\right)\right) \tag{3.28}$$

3.3 Results and analysis

The QD system considered has a cylindrical geometry structure, with a radius of $R = 8$ nm and a length of L = 10 nm; the calculations are made considering the parameters of a semiconductor QD of GaAs/$Ga_{0.6}$ $Al_{0.4}As$ [53]. Therefore, the following times are used, $T_1 = 1$ ps and $T_2 = 0.2$ ps, which are the times associated with spontaneous emission and decoherence, respectively [54].

The optical rectification coefficient χ_0 as a function of the incident photon energy,

in a cylindrical QD (CQD) with height L = 10 nm and radius R = 8 nm is shown in Fig. 3.1, for five different values of incoherent pumping in the weak pumping regime (ie: $P < \gamma$). Where it can be easily seen that in the weak pumping regime the optical rectification intensity decreases with the increase in pumping, keeping the resonance peak constant. Similar behavior was reported by Ref. [55]. The physical reason for this behavior is because incoherent pumping modifies the population of charge carriers in the nano-structured system without affecting the quantum energy levels of the system.

To investigate the effect of an incoherent pumping P on the optical response, it is plotted in Fig. 3.2 the maximum intensity of the optical rectification coefficient $\chi^{(2)}_{0,max}$ as a function of incoherent pumping. It is observed that as P increases in the weak regime (i.e.: $P/\gamma < 1$), the resonance peak decreases and it is zero when P = γ. However, in the strong pumping regime (i.e.: P/$\gamma > 1$), the intensity of the resonant peak of the optical rectification increases until it reaches a saturation value. This behavior occurs because $\chi^{(2)}_0$ is proportional to the term $(\rho^{(0)}_{gg} - \rho^{(0)}_{ee})$, the so-called quantum system population inversion as shown in Eq. (3.28), and, according to Chen et al. [56], the increase in the incoherent pumping rate P produces a decrease in the population of the ground state, while the population in the excited state increases. That is the reason that when P = γ the population equilibrium condition is met, $\rho^{(0)} = \rho^{(0)}_{ee}$, in which case the optical response is zero, since all resonant quantum levels are occupied. In the saturation state, the ground state is empty and the excited state is full. This condition will not change for incoherent pumping rate $P >> \gamma$.

3.4 Conclusions

In this work, an analytical expression was formally obtained for the optical rectification in a nanostructure through the solution of a Born-Markov master equation in the Lindblad form, considering as environment for the system the quantum vacuum of the electromagnetic field and taking into account the processes of spontaneous emission, dephasing, and incoherent pumping of excitons between two levels of the quantum system. It was found that incoherent pumping of excitons on the nanostructure: i) does not affect the energy separation of the levels of the quantum system and ii) produces population inversion. Also, it was found that in the weak pumping regime the intensity of the optical response decreases with the increase of incoherent pumping, while in the strong pumping regime the optical response increases until it is saturated when the excited state is full.

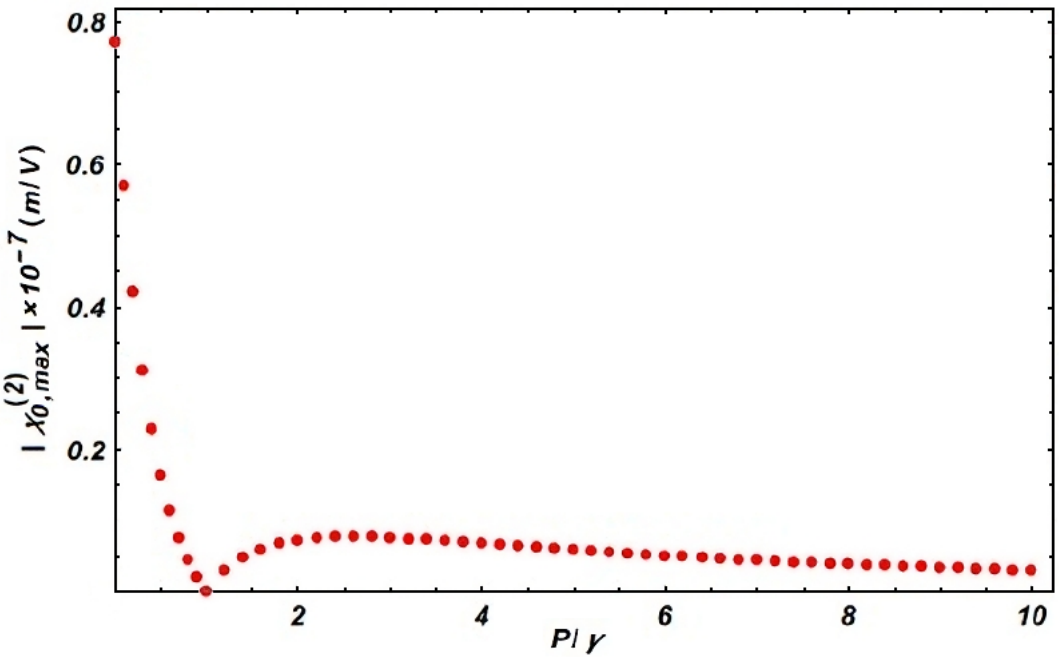

Figure 3.2 – Maximum optical rectification coefficient $\chi^{(2)}_{0,max}$ is plotted as function of P/γ, for a cylindrical QD with height L = 10 nm and radius R = 8 nm. $P/\gamma < 1$ corresponds to weak pumping and $P/\gamma > 1$ to strong pumping.

4 Magnetic Field Effects for the Emission Spectra in a Microcavity-Quantum Dot System

The behavior of the photoluminescence spectra of a single quantum dot in a semiconductor microcavity is modeled numerically in the presence of an external and constant magnetic field. The dynamics of the density operator is calculated using the master equation in the Lindblad form for decoherence processes: spontaneous emission, losses trough cavity mirrors, and dephasing. An incoherent pumping of excitons is used to feed the system. It is found in the photoluminescence spectra that for magnetic fields lower than ~ 2 T the system is in the strong coupling regime and for magnetic fields greater than 2 T the system emits light like three independent systems. The line that uncouples faster is the σ_- line.[1]

4.1 Introduction

The development of semiconductor physics at the experimental level made possible the creation of materials that confine electric charge in one, two or three dimensions. This has been achieved thanks to the development of epitaxial techniques for the growth of materials [57–61] and advanced lithographic techniques. In addition, these same techniques allow the control of the density of light states inside a semiconductor through spatial variations of the dielectric function, creating the cavity effect for electromagnetic radiation [62, 63].The creation of this type of physical systems that combine electronic and photonic confinements has allowed the possibility of studying and testing the quantum electrodynamics of cavities in systems other than atomic systems [64]. In the specific case of three-dimensional electric charge confinement, the structure called quantum dot (QD), immersed in a semiconductor microcavity (MC), coupling phenomena between these systems are evident [65, 66]. For example, in the emission spectrum of a MC-QD system, spontaneous emission can be modified or even inhibited if the system is in one of the strong or weak coupling regimes depending on the fabrication of the system [67–70].

An analysis of these emission processes allows the study of not only the electronic properties inside the QD, but also to determine some of the characteristics of the light emitted by the system, such as its quantum state and degree of radiation-matter coupling, among others [71].

[1] Published at http://www.revistacubanadefisica.org/index.php/rec/article/view/RCF_2018_35_115

A constant magnetic field applied to a QD affects its emission frequency, a fact that affects the shape of the full emission spectrum of the MC-QD system [72], therefore the variations of a magnetic field external to the system could be used as a control parameter of the emission spectrum. This is important in the implementation of quantum optics protocols; quantum teleportation protocol [73], development of single photon emission or detection technologies [74].

In section 4.2 the model of the system to be studied is formulated, in section 4.3 the dynamics of the system are proposed, in section 4.4 the results are presented and in section 4.5 the conclusions are presented.

4.2 Model

The behavior of the photoluminescence (PL) spectrum of a QD immersed in a MC is studied in the presence of an external magnetic field applied parallel to the confinement direction (see fig.4.1). The QD is considered as a two-level system and the MC with a single oscillation mode. This system is modeled as a modified version of the Jaynes-Cummings Hamiltonian [9] where an external magnetic field produces Zeeman and diamagnetic effects in the QD modifying the behavior of the emission lines of the entire system [72].

Figure 4.1 shows the sketch of the MC-QD physical system in the presence of an external magnetic field. Similar to a real one-dimensional cavity, the confinement effect is achieved using Bragg mirrors and the QD is located at the center of the microcavity. Dissipative processes are not shown in this sketch.

The Hamiltonian in the rotating wave approximation is written as [49, 75, 76]:

$$H_{RWA} = \hbar\omega_c \hat{a}^\dagger \hat{a} + \hbar\omega_{Q.D.} \hat{\sigma}^\dagger \hat{\sigma} + \hbar g(\hat{\sigma}\hat{a}^\dagger + \hat{\sigma}^\dagger \hat{a}), \tag{4.1}$$

where $\hbar\omega_c$ is the cavity resonance energy, $\hbar\omega_{Q.D.}$ is the separation energy between (two) levels of the QD, $\hbar g$ is the coupling energy between the MC and the QD, a represents the photon annihilation operator, σ the excitation annihilation operator in matter. Specifically, the separation energy between levels of the QD is modeled as: $\hbar\omega_{QD} = \hbar\omega_{QD}(0) \pm \frac{1}{2}\alpha\mu_B B + \beta \times 10^{-3} B^2$, where $\hbar\omega_{QD}(0)$ is the separation energy between states of the QD when the magnetic field is zero; The summands after the $\pm$ sign represent the Zeeman effect, where the QD's emission line splits into two (lines denoted by σ_+ and σ_-); and the diamagnetic effect, where the emission lines shift toward the blue. These effects exist under nonzero positive magnetic fields. The constants $\alpha = 2.9$ and $\beta = 0.6$ are used to fit the calculations for an InAs/GaAs QD [72] and μ_B is the Bohr magneton.

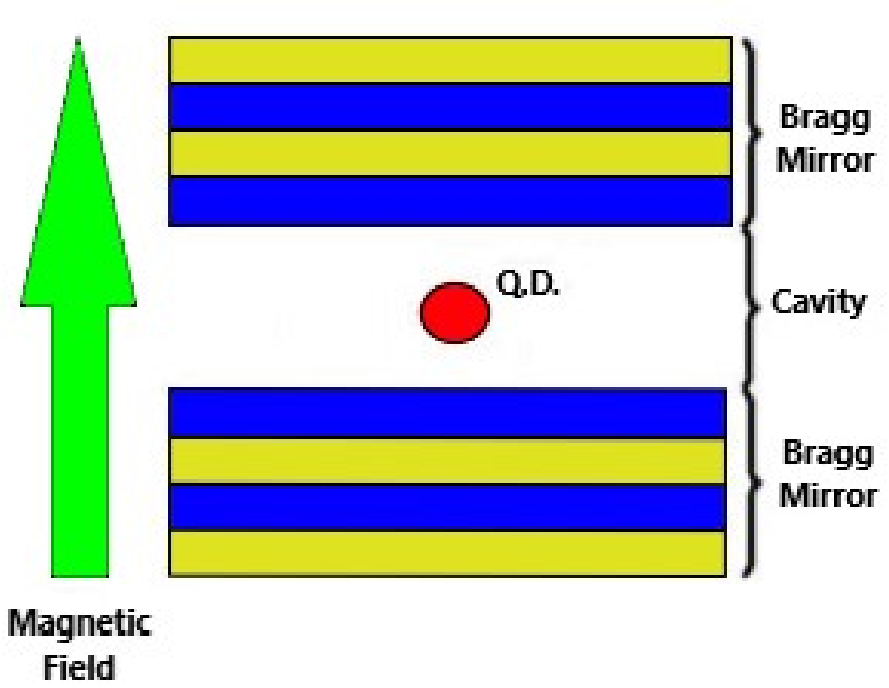

Figure 4.1 – Sketch of the quantum dot physical system immersed in a one-dimensional microcavity.

4.3 Dynamics

To describe in a more realistic way the dynamics of a QD-MC system it is necessary to consider both the evolution that comes from the Hamiltonian operator and the interaction with its environment. For this we will use the Lindblad formulation of the master equation written as [49, 75]:

$$\dot{\rho} = -\frac{i}{\hbar}[\rho, H_{RWA}] + L[\rho], \tag{4.2}$$

where ρ is the density operator of the system and L is the Lindblad operator that describes the dynamics of the system, composed of the sum of the operators that describe relaxation processes in the system such as: cavity losses $\kappa(2a\rho a^\dagger - a^\dagger a\rho - \rho a^\dagger a)$, spontaneous emission $\gamma(2\sigma\rho\sigma^\dagger - \sigma^\dagger\sigma\rho - \rho\sigma^\dagger\sigma)$, phase shift $\frac{1}{2}\gamma_\phi(\sigma_z\rho\sigma_z - \rho)$, in addition to the incoherent exciton pumping process in the QD $\frac{1}{2}P\left(2\sigma^\dagger\rho\sigma - \rho\sigma\sigma^\dagger - \sigma\sigma^\dagger\hat{\rho}\right)$.

The solution to this system was implemented in the Python language with the QuTip extension [77],developed to solve the dynamics of open quantum systems. For the calculation of the photoluminescence spectrum the expression

$$S(\omega) = \int_{-\infty}^{\infty} \lim_{t\to\infty} \left\langle a^\dagger(t+\tau)a(t)\right\rangle e^{-i\omega\tau} d\tau \tag{4.3}$$

[76], is used, which is the Fourier transform of the two-times correlation function

$$\left\langle a^\dagger(t+\tau)a(t)\right\rangle = Tr(a^\dagger(t+\tau)a(t)\rho), \tag{4.4}$$

this calculation is solved in Qutip using the command “spectra" [77].

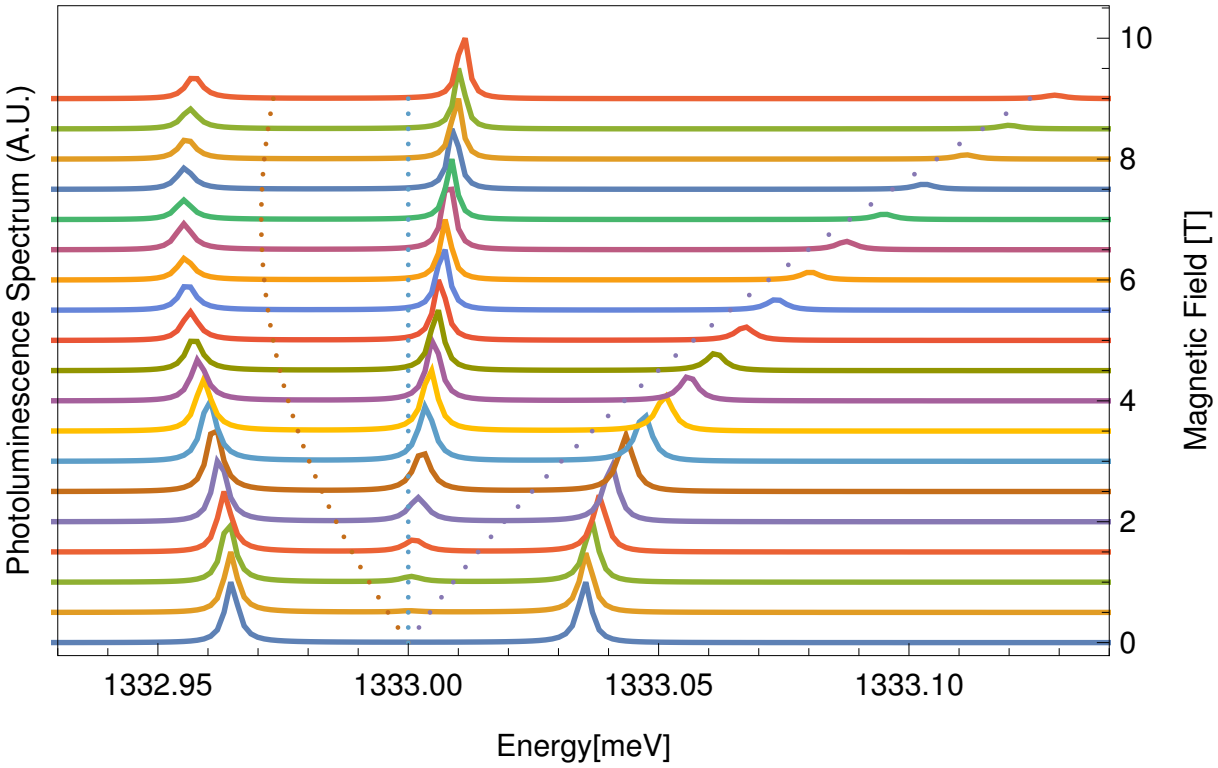

Figure 4.2 – Photoluminescence spectrum of a QD-MC system for different values of constant magnetic field. The dotted lines from left to right represent the behavior of the QD lines (σ_+, σ_-) and the cavity that the system should follow in the presence of a magnetic field when the quantum dot is decoupled from the cavity.

4.4 Results and discussion

The necessary parameters used to make the calculations were the cavity energy $\hbar\omega_c = 1333.0$ meV [72], the initial separation of the QD energy levels $\hbar\omega_{Q.D.}(0) = 1333.0$ meV [72],the radiation-matter coupling parameter $\hbar g = 25 \times 10^{-3}$ meV, the cavity dissipation rate $\kappa = 1.0 \times 10^{-3}$, the dissipation rate of the QD excitation $\gamma = 1.0 \times 10^{-3}$, the phase shift term $\gamma_\phi = 1 \times 10^{-3}$ and the incoherent pumping rate of excitations $P = 1.0 \times 10^{-6}$.

Figure 4.2 shows the photoluminescence spectrum as a function of emission energy of a QD-MC system in the presence of a constant external magnetic field and the behavior of the QDs in the presence of an external magnetic field applied parallel to the cavity confinement direction, for magnetic fields from zero to 9 T, in increments of 0.5 T. In Figure 4.2, it is observed that for magnetic fields less than ~ 2 T the typical behavior of the luminescence spectrum associated with a coupled system is obtained; where two peaks are found in the luminescence spectrum. This is because magnetic fields of intensities less than ~ 2 T maintain the coupling between the emission lines of the QD and the MC, however when the magnetic field is increased the system is no longer in resonance, therefore

the coupling disappears and thus the system behaves as three independent emitters; cavity, σ_+ emission line and σ_- emission line for the QD. The physical reason for this behavior is due to the Zeeman effect induced by the interaction of the system with the external magnetic field, this effect is evidenced because a breaking of the degeneracy of the system is observed. However an asymmetry is also observed between the central line and the lateral lines due to the Zeeman and diamagnetic terms defined in the Hamiltonian of the QD.

4.5 Conclusions

In this work, the behavior of an MC-QD system in the presence of an external magnetic field was studied. It was found that from a value of magnetic field greater than approximately 2 T there is decoupling between the emission lines of the system. It is shown that the σ_- line of the QD decouples more rapidly with the cavity.

5 Weak to strong coupling conditions for a microcavity-quantum dot system under incoherent pumping

We theoretically study the power spectra of a microcavity-quantum dot system under incoherent pumping of photons and excitons, considering two models: one with linked cavity loss rate and pumping, and one with independent cavity loss rate and pumping. We investigate the transition from strong to weak coupling under low and high incoherent pumping in each model and determine sets of parameters necessary to achieve these regimes of light-matter interaction. Despite their differences, both models exhibit a sequence of transitions between weak, strong, and weak coupling as the pumping is increased. This prediction has not yet been observed, before this work.[1]

5.1 Introduction

The development of the physics of semiconductor heterostructures has allowed greater control of the optical and electrical properties of semiconductor devices [78–82]. With these achievements, it is possible to control charge confinement at the nanoscale in several dimensions. A semiconductor structure that confines the charges in all three dimensions at the nanometer scale is usually called a “quantum dot" [5, 13, 83, 84]. On the other hand, in the case of light, it is possible to develop semiconductor heterostructures that modify the diffraction index to confine light to regions with the order of its wavelength [2, 16, 63, 85]. The combination of these technological developments has allowed the investigation of quantum electrodynamics phenomena within the realm of solid-state physics and brought the area of quantum optics, where light-matter coupling is a very important topic, within the domain of semiconductor physics. For the specific case of heterostructures that constitute optical nanocavities with embedded quantum dots, two kinds of light-matter coupling have been identified, the weak coupling [86, 87] and the strong coupling [8, 88–90] regimes. In the weak coupling regime, the interaction between light (photons in the cavity mode) and matter (the excitons in the quantum dots) is relatively weak, compared to the individual incoherent rates of creation (pumping) and annihilation (decay). In this regime, the light and matter dynamics are nearly independent and can be satisfactorily described separately. Conversely, the strong coupling regime involves a significant coherent energy exchange between the exciton and a single cavity mode, necessitating the description

[1] Published at Physica B 591, 416282 (2024) https://doi.org/10.1016/j.physb.2024.416282

of the system in terms of a new set of quantum states of the light-matter system, the hybridized *polariton* states. This regime exhibits a characteristic splitting of the energy levels at resonance, visible in the emission (photoluminescence) spectra. Changes in the pumping or decay rates alter the coupling conditions, as explored by Laussy et al. [91], Del Valle and Laussy [92] and others, and as it will be further discussed in this work.

To achieve experimentally the regime of strong coupling in this system was initially a challenge due to the difficulty of obtaining an optical cavity with a high-quality factor and with quantum dots tuned spatially and spectroscopically to one of the cavity modes. It was the work of Reithmaier et al. [67] and Yoshie et al. [68] that demonstrated for the first time strong coupling in an optical cavity with embedded quantum dots, for the case of a micropillar and a photonic crystal, respectively. Due to their optical properties of recombination of electron-hole pairs, with a large separation between energy levels, quantum dots are in general modeled as a two-level system. And, usually, only one photonic mode of the cavity needs to be considered, the mode which is close to resonance to the two-level quantum dot. Under several approximations, it is possible to use the theory of open quantum systems to describe this kind of system, where a Lindblad master equation has to be solved [29, 91, 93, 94]. This equation includes rates of loss through cavity mirrors, spontaneous emission, and pumping rates in the cavity and in the matter modes, in an effort to describe the system more realistically. One observable quantity that can be obtained from the solution of this master equation, and correlation theory, is the power spectra. Laussy et al. [91] report the dependence of the spectra of a system of a quantum dot embedded in an optical cavity on several of the above-mentioned parameters. The conditions for weak coupling, non-resolution strong coupling, and strong coupling were investigated as a function of exciton pumping (P_x) and cavity loss (Γ_c), for a set of values expressed as multiples of the coupling term. Questions such as how the characteristics of the rate of pumping of excitons affect the power spectra have been studied by Poddubny et al. [95], who investigated the emission spectra of quantum dots coupled to a cavity under variation of the pumping of excitons. It was pointed out that the form of the emission spectrum depends strongly on the pumping of excitons parameter, P_x. Analytical results describing the effect of pumping on the coupling regime were provided by Elena Del Valle [96].

Some studies similar to the idea of strong-to-weak coupling transition have been reported in [97–107]. In the work reported in this chapter, we study theoretically the emission spectra of a coupled cavity-quantum dot system in the strong and weak coupling regimes, under various conditions of photon and exciton losses and pumpings, for two similar theoretical models, one in which the cavity loss rate and the pumping are linked, and another where they are independent. We show that in the resonance condition for each model, the pumping of photons in the cavity is a determinant parameter for the shape of the photoluminescence (PL) spectra, which clearly reveals the regime of light-matter

coupling in which the system is located. Also, for our sets of parameters, we found that for an increasing cavity pumping P_c, it is possible to start from an initial weak coupling condition, pass through a strong coupling region, and then return to a weak coupling condition. This is an interesting effect that must be carefully considered in experimental work. We also show that in some situations, a minimal level of photon pumping is required to achieve the strong coupling regime.

5.2 Model

We describe a system comprising a microcavity with one embedded quantum dot, considering both exciton and photon pumping, as well as processes involving the loss of photons and matter decay.

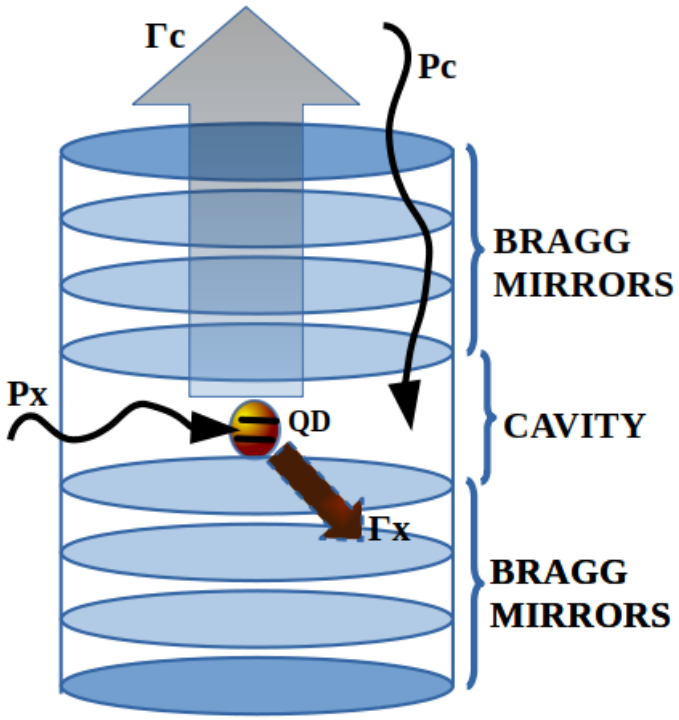

Figure 5.1 – Schematic representation of the system with a quantum dot immersed in a cavity. It illustrates processes such as cavity photon pumping (P_c), exciton pumping (P_x), loss of photons from the cavity (Γ_c), and spontaneous emission (Γ_x) rates of the QD exciton.

Figure 5.1 shows the system representation, where a quantum dot is situated within an optical microcavity bounded by Bragg mirrors. Lateral light confinement occurs through total internal reflection, similar to a micropillar [67, 108]. Schematic representations of light and exciton pumpings (P_c and P_x, respectively), as well as dissipation processes, including photon loss from the cavity (Γ_c) and spontaneous emission (Γ_x), are provided.

5.2.1 System Hamiltonian

The Hamiltonian in this work describes a quantum dot-cavity system, modeling the exciton associated with the quantum dot as a two-level system, with $|G\rangle$ for the ground state and $|X\rangle$ for the exciton state (bound state of an electron–hole pair), within a cavity with a single mode frequency ω_c:

$$H = \hbar\omega_x \hat{\sigma}^\dagger \hat{\sigma} + \hbar\omega_c \hat{a}^\dagger \hat{a} + \hbar g(\hat{\sigma}^\dagger \hat{a} + \hat{\sigma}\hat{a}^\dagger). \tag{5.1}$$

The parameter ω_x denotes the ground to excited state exciton transition frequency, associated with the operator $\hat{\sigma}^\dagger = |X\rangle\langle G|$. The cavity mode frequency is represented by ω_c, corresponding to the photon creation operator $\hat{a}^\dagger$. The coupling between the cavity mode and the exciton is described by the parameter g. The rotating wave approximation is employed, leading to the Jaynes-Cummings model [9, 10, 108], and section 2.1.1 for this system.

5.2.2 Dynamics

In order to obtain the dynamics we employ the theory of open quantum systems, making use of the Born-Markov approximations [49, 109, 110], and section 2.3. This approach enables us to describe losses and pumping effects by formulating a master equation for the density matrix in the Lindblad form (with $\hbar = 1$):

$$\frac{d\rho}{dt} = -\imath[H, \rho] + \mathcal{L}(\rho). \tag{5.2}$$

Here, H represents the full Hamiltonian [Eq. (5.1)], and $\mathcal{L}(\rho)$ denotes the Lindblad superoperator, encompassing the incoherent part of the density matrix. We consider and compare two different models for the Lindblad superoperator: Model A, used in Refs. [95, 111],

$$\begin{aligned}\mathcal{L}_A(\rho) = {} & P_c\mathcal{D}[a^\dagger] + \Gamma_c\mathcal{D}[a] \\ & + P_x\mathcal{D}[\sigma_+] + \Gamma_x\mathcal{D}[\sigma_-],\end{aligned} \tag{5.3}$$

and Model B, utilized in Refs. [112, 113],

$$\begin{aligned}\mathcal{L}_B(\rho) = {} & P_c\mathcal{D}[a^\dagger] + (\Gamma_c + P_c)\mathcal{D}[a] \\ & + P_x\mathcal{D}[\sigma_+] + \Gamma_x\mathcal{D}[\sigma_-].\end{aligned} \tag{5.4}$$

In both models, $\mathcal{D}[L] = L\rho L^\dagger - \frac{1}{2}(L^\dagger L\rho + \rho L^\dagger L)$ is the Lindblad operator, P_c and Γ_c represent the incoherent cavity pump and cavity loss, while P_x and Γ_x signify the incoherent quantum dot pump and quantum dot losses, respectively, as schematically depicted in Fig. 5.1. The primary distinction between the models lies in how incoherent pumping affects the cavity losses. Model B assumes that the number of photons in the cavity affects directly the decay rate of the cavity mode. In this way, for Model B, pumping photons into the cavity directly increases the cavity mode's decay rate. Conversely, for Model A, there is no dependence of the decay rates on the cavity photon population. As it will be seen in Section 5.3, both models predict similar results for the dynamics of the system, although Model A presents some convergence issues in the simulation of the power spectra. We neglect pure dephasing to focus on the effects of different pumping models. As we increase the pump power, we anticipate a transition from strong to weak coupling, as observed in Ref. [114].

To solve for the system's density matrix, it is expanded in a combined Fock and exciton basis $|\psi\rangle = \sum_{n,s} |n\rangle |s\rangle$ truncated at N_{cut}. The suitability of this expansion is assessed by examining the steady-state cavity occupation $\langle a^\dagger a\rangle_{ss} = \text{Tr}\left(\rho_{ss} a^\dagger a\right)$.

One important difference of the two models is that there is no convergence for model A when the pumping of the cavity is greater than the cavity loss, $P_c > \Gamma_c$, as we can see in Fig. 5.2. For this figure we use $N_{\text{cut}} = 500$ and increase the pumping of the cavity for $\Gamma_c = 4\ g$, $\Gamma_x = 0.2\ g$, and $P_x = 0.2\ g$. These are some of the parameter values that we will use in this work.

Notice that when $P_c > \Gamma_c$, the occupation of the cavity in Model A (solid red line) goes to the value of N_{cut}, which is a clear indication that the system does not converge for that choice of parameters. In fact, as the gain is greater than the loss, this is an expected result. Model B demonstrates a higher degree of stability in terms of the cavity occupation number.

5.2.3 Power spectra

One of the observables that allows us to analyze the light-matter interaction is the power spectrum, due to its property to distinguish the energy distribution available in the system [109]. The power spectrum $S(\omega)$ is defined as the real part of the Fourier transform of the mean values of the two-time correlation function of the photon operator,

$$S(\omega) = Re \int_0^\infty e^{-i\omega t} \langle a^\dagger(t) a(0)\rangle dt. \tag{5.5}$$

The power spectrum serves as a visual tool for analyzing the system and distinguishing between strong and weak coupling conditions. In resonance, a clear splitting in the power spectra curves indicates a strong coupling condition. Variations in parameters lead to changes in the photoluminescence (PL) spectra. Both types of pumping can modify

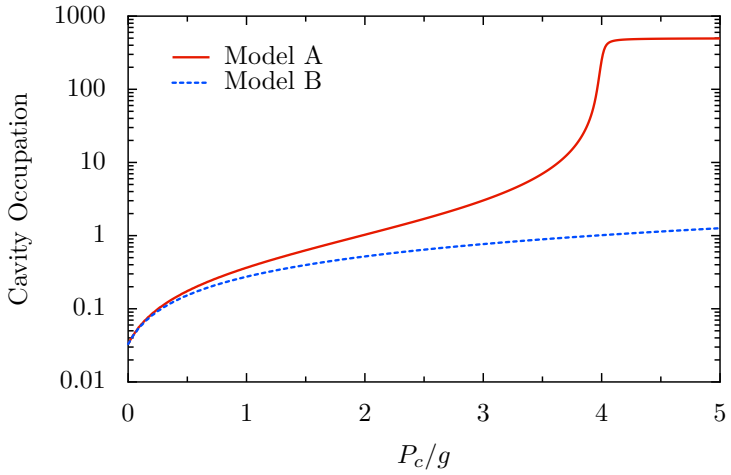

Figure 5.2 – Cavity occupation as a function of cavity pumping rate (P_c) at resonance ($\omega_c = \omega_x$) for $\Gamma_c = 4\ g$, $\Gamma_x = 0.2\ g$, and $P_x = 0.2\ g$. The solid red line is for Model A and the blue dashed line is for Model B. Model A does not converge when $P_c > \Gamma_c$. We used $N_{\text{cut}} = 500$.

the PL, not only in terms of emission intensity but also in terms of driving the system into either strong or weak coupling regimes, as reported by Laussy et al. [91].

Spectrally, each regime is distinguishable in the system's emission spectra. Weak coupling exhibits a single curve, while intermediate coupling displays a single curve with a distinctly flat top. Strong coupling is characterized by a clear splitting of the emission line.

5.3 Results and Analysis

5.3.1 Power spectra for Model A

In this part, we investigate the spectral characteristics of transitions in Model A, defined by equation (5.3). Figures 5.3(a),(b) show the Fourier transform of the correlation function from Eq. (5.5), each with a specific set of parameters: pumping strengths (P_c and P_x), decay terms (Γ_c and Γ_x), and the light-matter coupling term, g. Figure 5.3(a) depicts spectra for $\Gamma_c = 4.0\ g$, with increasing cavity pumping P_c. As P_c increases, the spectra transition from a single peak (weak coupling) to a flat-topped curve (intermediate coupling) to two distinct peaks (strong coupling), and finally back to a single peak (weak coupling). For this high-loss cavity $\Gamma_c = 4.0\ g$, strong coupling occurs between $P_c \sim 0.5\ g$ and $P_c \sim 2.0\ g$. Figure 5.3(b) shows similar coupling regime transitions as a function of Γ_c, with constant $P_c = 0.3\ g$. Strong coupling is observed between $\Gamma_c \sim 0.5\ g$ and $\Gamma_c \sim 4.0\ g$. This sequence of coupling transitions (from weak to strong and then weak coupling again), induced by varying pumping power relative to cavity loss, is a novel observation. It reveals that for high-loss cavities, a certain level of cavity pumping is required to achieve strong coupling, but excessive pumping can disrupt this condition.

Figure 5.3(c) depicts a map of P_c as a function of Γ_c for Model A, constructed by quantifying the number of peaks in the spectra across the parameter space. This mapping serves as a tool to identify the dynamics within the cavity-quantum dot system. It establishes correlations between observed spectral characteristics in regions of strong and weak coupling under different external pumping conditions and cavity types. This enables the categorization and differentiation of the various coupling regions. The white region in the map ($P_c > \Gamma_c$) cannot be analyzed due to model convergence issues.

While the transition between strong and weak coupling has been studied in several works for model A, it is important to note that most have treated the problem in the low-excitation limit, where the equations of motion for the operators can be approximated and an analytical solution is possible. In this context, the Rabi splitting was obtained by Laucht *et al.* [114] and del Valle *et al.* [115], whose equation can be written as $\Omega = \sqrt{g^2 - (\lambda_x - \lambda_c)^2}$, where $\lambda_x = (\Gamma_x + P_x)/4$ and $\lambda_c = (\Gamma_c - P_c)/4$. This model only predicts two peaks in the spectra that become one when the Rabi splitting goes to zero, a condition in which the Rabi splitting becomes a purely imaginary number. We can then use this equation to predict the strong-to-weak coupling transition.

In Fig. 5.4(a), we plot the real and imaginary parts of the Rabi splitting as a function of cavity loss for $P_c = 0.1\ g$ and other parameters being the same as those used in Fig. 5.3. We observe a strong-to-weak coupling transition close to $\Gamma = 5\ g$, in qualitative agreement with the result presented in Fig. 5.3(c), that presents a transition from two to one peak around to $\Gamma = 4\ g$. In Fig. 5.4(b), we plot the real and imaginary parts of the Rabi splitting as a function of cavity pumping for $\Gamma = 5\ g$. For low pumping, we see that the result also qualitatively agrees with the result of Fig. 5.3(c), where we have a weak-to-strong coupling transition, but the model fails to describe a new strong-to-weak coupling transition, seen in the upper part of Fig. 5.3(c). This is because the Rabi equation was obtained in the linear regime, and is not valid for high pumping.

Figure 5.5 presents a similar spectral analysis using Model A, but with fixed cavity pumping $P_c = 0.1\ g$, focusing on the dependence on exciton pumping P_x. Figure 5.5(a) shows spectra for a low-loss cavity ($\Gamma_c = 0.3\ g$) and increasing P_x. The spectra gradually evolve from strong coupling at low P_x to weak coupling with a single peak for $P_x \gtrsim 0.5\ g$. Interestingly, the initial spectra for very low P_x exhibit multiple peaks, a situation that changes rapidly with increasing P_x. These multiple peaks come from transitions involving states with more than one excitation [115].

Figure 5.5(b) shows spectra for fixed $P_c = 0.1\ g$, $P_x = 0.5\ g$, and increasing cavity loss Γ_c. For low Γ_c, the single-peak weak coupling regime is observed. As Γ_c increases, the spectra transition to intermediate coupling, then to two peaks, and finally back to a single peak for high Γ_c. Similar to Figure 5.3, a sequence of weak-to-strong-to-weak coupling transitions is observed, but this time with varying exciton pumping. The strong coupling

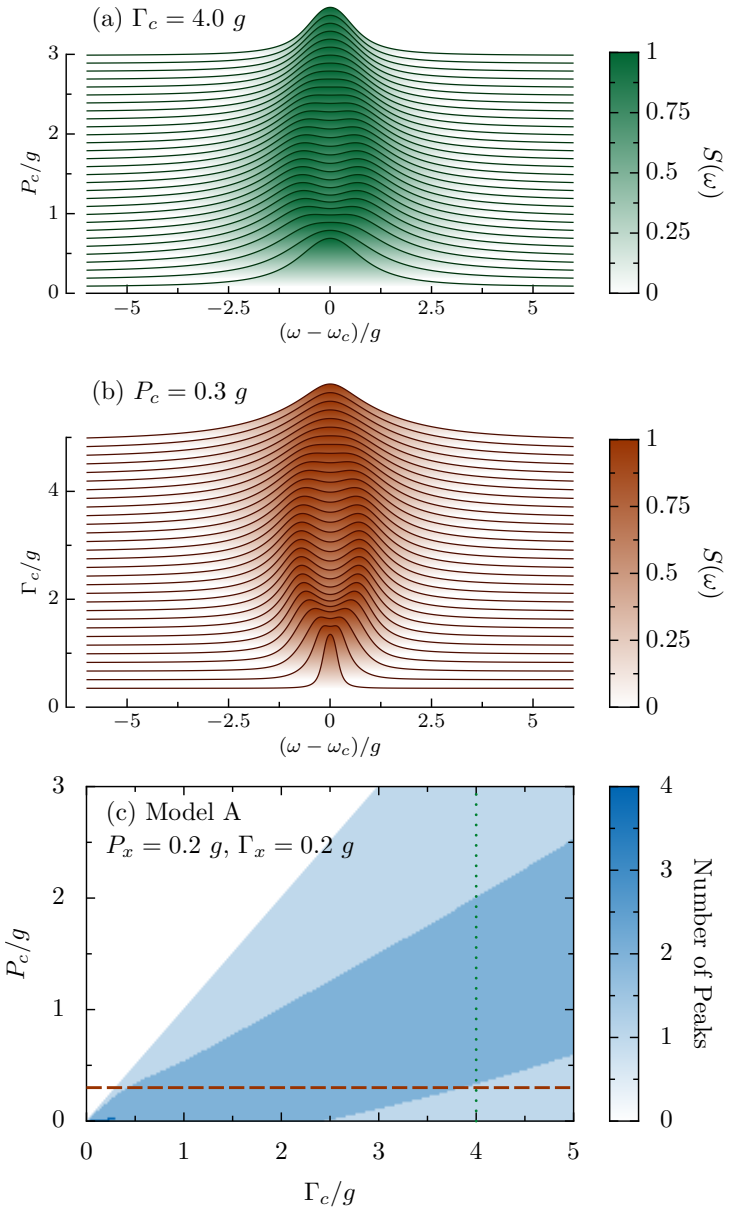

Figure 5.3 – Spectral analysis for Model *A*. (a) Normalized spectra as a function of cavity pumping rate P_c at resonance ($\omega_c = \omega_x$), for $\Gamma_c = 4\ g$. (b) Normalized spectrum as a function of cavity loss rate Γ_c, at resonance, for $P_c = 0.3\ g$. (c) Number of peaks (color map) as a function of P_c and Γ_c at resonance, determining weak/strong coupling regions. Zero peaks (white region): model does not converge ($P_c > \Gamma_c$), one peak (light blue): weak coupling, two or more peaks (darker blue): strong coupling. The spectra shown in panels (a) and (b) correspond to the parameters of the dotted and dashed lines of the panel (c), respectively. Other parameters: $\Gamma_x = 0.2\ g$, $P_x = 0.2\ g$. For (a) and (b), $N_{\text{cut}} = 30$, for (c), $N_{\text{cut}} = 15$.

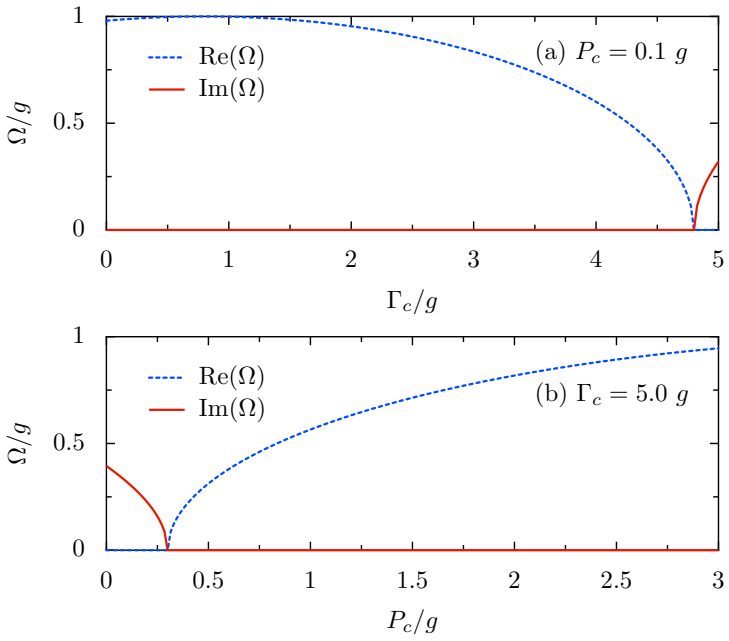

Figure 5.4 – (a) Real and imaginary parts of the Rabi splitting as a function of cavity loss for $P_c = 0.1\ g$ and other parameters being the same as those used in Fig. 5.3. (b) Real and imaginary parts of the Rabi splitting as a function of cavity pumping for $\Gamma = 5\ g$.

regime is observed for $\Gamma_c \sim 0.6\ g$ to $\Gamma_c \sim 2.0\ g$ at $P_x = 0.5\ g$.

Figure 5.5(c) maps P_x as a function of Γ_c, quantifying the number of peaks in the spectra. This map complements the coupling regimes predicted by Model A. The dark blue region indicates strong coupling, while the light blue region indicates weak coupling. A small region with multiple peaks is seen at the lowest P_x and Γ_c values. Again, the white stripe for $\Gamma_c < P_c$ cannot be considered due to convergence issues with Model A.

5.3.2 Power spectra for Model B

We now shift our focus to the spectral characteristics of the cavity-quantum dot system within the framework of Model B, as defined by equation (5.4). Figures 5.6(a), (b) showcase a series of normalized spectra for the microcavity-quantum dot system at resonance, calculated using Model B.

Figure 5.6(a) shows the spectra for a high loss cavity, $\Gamma_c = 3.5\ g$, for increasing values of cavity pumping, ranging from zero up to $P_c = 5\ g$. Figure 5.6(b) presents a set of spectra, also calculated using Model B, for a constant value of cavity pumping, $P_c = 0.5\ g$, and increasing values of cavity decay Γ_c. As observed with Model A, a sequence of coupling regime transitions, weak-strong-weak coupling, is evident as the pumping power is varied relative to the cavity loss. This implies that achieving the strong coupling condition necessitates a delicate tuning of parameters. Excessive pumping power disrupts the strong

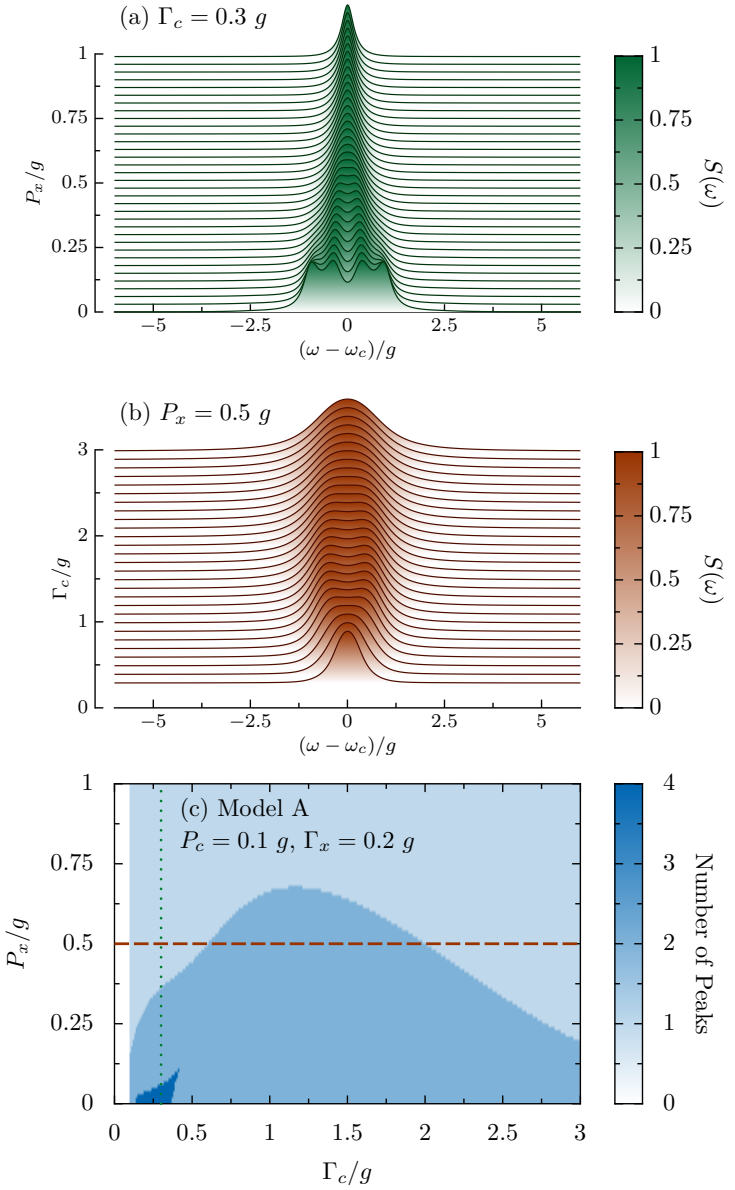

Figure 5.5 – Spectral analysis for exciton pumping, with Model A: (a) Normalized spectra as a function of P_x at resonance ($\omega_c = \omega_x$) for $\Gamma_c = 0.3\ g$; (b) Normalized spectra as a function of Γ_c at resonance for $P_x = 0.5\ g$; (c) Number of peaks (color map) as a function of P_x and Γ_c at resonance determining weak/strong coupling boundary regions. Zero peaks (white region): model does not converge ($P_c > \Gamma_c$), one peak (light blue): weak coupling, two or more peaks (dark blue): strong coupling. The spectra shown in panels (a) and (b) correspond to the parameters of the dotted and dashed lines of the panel (c), respectively. Other parameters are $\Gamma_x = 0.2\ g$ and $P_c = 0.1\ g$. For (a) and (b) we use $N_{\text{cut}} = 30$ and for (c) $N_{\text{cut}} = 15$.

coupling, a well-established phenomenon. However, our results further demonstrate that for relatively high-loss cavities, a certain amount of pumping might be required to observe the cavity-quantum dot system in the strong coupling regime. For the parameters used in Fig. 5.6(a), a region of strong coupling is identified for a range of cavity pumping values between 0.4 g and 2.8 g, approximately. In the case of the set of parameters used for Figure 5.6(b), strong coupling is observed for 0.5 $g \leq \Gamma_c \leq 3.5$ g, approximately.

The P_x as a function of Γ_c map presented in Fig. 5.6(c), created by quantifying the number of peaks within numerous spectra calculated using Model B, further highlights the need for parameter tuning to achieve the desired coupling regime. The result is similar to that obtained using Model A, but for Model B, we do not encounter convergence issues, allowing for confident determination of the coupling regime from the spectra even in situations with $P_c > \Gamma_c$. The main feature, that for poor-quality cavities (high Γ_c), a certain amount of pumping is required to attain the strong coupling condition, is also predicted by Model B, as evident from comparing Figures 5.3(c) and 5.6(c). Model B predicts a slightly higher value of cavity pumping for a high Γ_c cavity to achieve strong coupling compared to Model A, but the overall characteristics of the results are consistent between the two models.

In summary, our results overall indicate that to achieve the strong coupling regime, revealed in the PL spectra by the splitting of the emission peak, one needs a delicate balance of the populations of excitons and photons in the system. At low pumping power, we believe that we see only one peak in the spectral function due to an insufficient cavity population hindering coherent exchange between the cavity mode and the exciton. As the power increases, this coherent exchange becomes possible, and we observe a double peak in the PL spectra. Further pumping induces a loss of coherence, because the injected photons lack a defined phase. Therefore, for high loss cavities, some degree of cavity pumping is mandatory in order to achieve strong coupling. On the other hand, high excitation power will revert the system to the weak coupling condition.

5.4 Conclusion

We investigate the emission spectra of a system comprising an optical cavity with an embedded quantum dot, specifically when the two-level system, i.e., the exciton in the quantum dot, is near resonance with the cavity. The emission lines are calculated for various values of incoherent photon pumping, exciton pumping, cavity loss, and spontaneous emission, using two distinct models for how incoherent pumping affects cavity losses. We utilize the shape of the spectral emission lines to indicate the prevailing coupling regime, strong or weak, for different sets of these parameters. Under certain conditions, particularly when photon loss in the cavity is relatively high, we find that a system initially in the weak

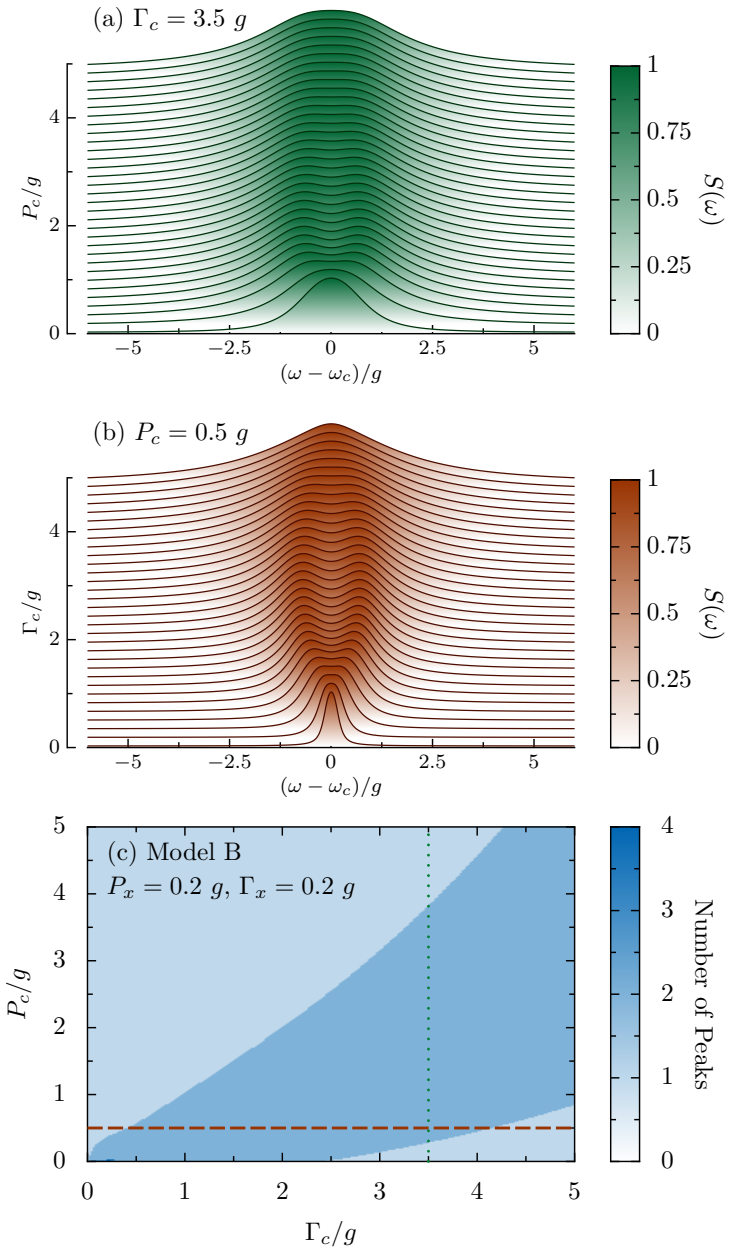

Figure 5.6 – Spectral analysis using Model B. (a) Normalized spectra for several values of cavity pumping rate P_c, for a high loss cavity, with cavity decay rate $\Gamma_c = 3.5\ g$. (b) Normalized spectra for increasing values of the cavity loss rate Γ_c, for a fixed rate of cavity pumping, $P_c = 0.5\ g$. (c) Number of peaks (color map) in the PL spectra as a function of P_c and Γ_c, at resonance. We use the number of peaks to determine the coupling regime regions. One peak: weak coupling, two or more peaks: strong coupling. The dotted and dashed lines show the parameter values chosen for the spectra shown in panels (a) and (b), respectively. Other parameters: $\Gamma_x = 0.2\ g$, $P_x = 0.2\ g$. For (a) and (b), $N_{\text{cut}} = 30$, for (c), $N_{\text{cut}} = 15$.

coupling regime can transition into the strong coupling regime as the photon pumping parameter increases. Further increase in incoherent photon pumping returns the system to the weak coupling regime. In other words, we demonstrate that achieving the strong coupling regime in an optical cavity-quantum dot system with a relatively high photon loss rate necessitates a certain level of photon pumping in the cavity. This pumping must be sufficient to induce strong coupling but not excessive, as excessive photon pumping disrupts the strong coupling condition.

As theoretically demonstrated by Laussy et al. [91], and verified by subsequent studies [92,95,116–119], specific inequalities can be established to delineate the boundaries between strong and weak coupling behavior. Notably, in regions where the exciton pumping satisfies the conditions $P_x < g^2/\Gamma_c$ and $P_x < g^2/\Gamma_c$, the strong coupling regime can be attained. Proposing similar equations in our model proves to be challenging, due to the high level of cavity pumping regimes we investigate. This leads to significant cavity mode occupation, as shown in Figure 2. Consequently, truncating the density matrix is not straightforward. For example, while Laussy's equations predict only two peaks, valid for lower pumping powers, our complete model captures the multi-peak scenarios shown in Figure 4(a).

In addition, our work reveals the existence of a non-trivial set of parameters for which the strong coupling condition emerges within a region of weak coupling in parameter space. This region arises for a parameter set that includes large values of Γ_c and the controlled cavity pumping term P_c. Our findings indicate that for certain parameter sets, an increase in cavity photon pumping P_c can lead to a transition from weak coupling to strong coupling. However, if P_c continues to increase, the system reverts back to weak coupling. This subtle effect has been observed using two distinct methods for modeling the influence of incoherent pumping on cavity losses in a quantum dot-cavity system within the framework of open quantum system theory.

In conclusion, this work demonstrates that a well-defined set of parameters (photon and exciton pumpings, cavity loss and spontaneous emission rates, photon-matter coupling strength) is crucial for enabling the strong coupling regime in an optical cavity-quantum dot system. We have mapped several parameter sets that yield strong coupling, providing guidance for experimentalists seeking to achieve this regime. As a general principle, strong coupling regions in parameter space are associated with high-quality cavities and strong photon-exciton coupling. For cavities with lower quality factors, maintaining a sufficiently high (but not excessive) rate of photon and exciton pumping is essential for reaching strong coupling.

6 General Conclusions

This thesis investigates various aspects of quantum systems, particularly focusing on the interaction between optical cavities and quantum dots (QDs), and the influence on these systems of external factors such as incoherent pumping and magnetic fields. Through analytical and numerical approaches, significant insights have been gained into the behavior of these systems across different coupling regimes.

The first study successfully derived an analytical expression for optical rectification in nanostructures under a quantum vacuum environment, highlighting the effects of incoherent exciton pumping. It was found that incoherent pumping induces population inversion without altering the energy separation of the quantum levels, and that the optical response varies with the pumping intensity—decreasing in weak pumping regimes and saturating under strong pumping conditions.

The second work explored the impact of an external magnetic field on a microcavity-quantum dot (MC-QD) system, revealing that above magnetic fields around 2 Teslas, the emission lines of the QD decouple from the cavity. Notably, the σ_- line showed a more rapid decoupling, providing valuable information about the magnetic field's role in modulating light-matter interactions in such systems.

The third study focused on the emission spectra of a cavity-QD system near resonance, demonstrating how incoherent photon and exciton pumping, cavity losses, and spontaneous emission affect the transition between weak and strong coupling regimes. It was shown that the system could transition into strong coupling under moderate photon pumping, even with high photon loss, but excessive pumping disrupts this condition, causing a reversion to weak coupling.

Together, these works contribute to a deeper understanding of light-matter interactions in quantum systems, emphasizing the delicate balance of external parameters required to control and enhance coupling behaviors. These findings open up potential avenues for optimizing the design and operation of quantum technologies, particularly in the fields of quantum optics and cavity quantum electrodynamics.

Bibliography

[1] Nielsen, M. e I. Chuang: *Quantum computation and quantum information*. Cambridge University Press, 2000. Quoted 2 times on pages 13 and 20.

[2] Sujecki, Slawomir: *Photonics modelling and design*. CRC press, 2018. Quoted 2 times on pages 13 and 38.

[3] Puers, Robert, Livio Baldi, Marcel Van de Voorde e Sebastiaan E. Van Nooten: *Nanoelectronics: Materials, Devices, Applications, 2 Volumes*. John Wiley & Sons, 2017. Quoted on the page 13.

[4] Orji, Ndubuisi G, Mustafa Badaroglu, Bryan M Barnes, Carlos Beitia, Benjamin D Bunday, Umberto Celano, Regis J Kline, Mark Neisser, Yaw Obeng e AE Vladar: *Metrology for the next generation of semiconductor devices*. Nature Electronics, 1(10):532–547, 2018. Quoted on the page 13.

[5] Terna, Augustine D., Elias E. Elemike, Justina I. Mbonu, Omosede E. Osafile e Rachael O. Ezeani: *The future of semiconductors nanoparticles: Synthesis, properties and applications*. Materials Science and Engineering: B, 272:115363, 2021. Quoted 2 times on pages 13 and 38.

[6] Goy, P.h., J.M. Raimond, M. Gross e S. Haroche: *Observation of cavity-enhanced single-atom spontaneous emission*. Physical Review Letters, 50(24):1903, 1983. Quoted on the page 13.

[7] Haroche, Serge: *Nobel Lecture: Controlling photons in a box and exploring the quantum to classical boundary*. Reviews of Modern Physics, 85(3):1083, 2013. Quoted on the page 13.

[8] Reithmaier, Johann Peter: *Strong exciton–photon coupling in semiconductor quantum dot systems*. Semiconductor Science and Technology, 23(12):123001, 2008. Quoted 2 times on pages 13 and 38.

[9] Jaynes, Edwin T e Frederick W Cummings: *Comparison of quantum and semiclassical radiation theories with application to the beam maser*. Proceedings of the IEEE, 51(1):89–109, 1963. Quoted 3 times on pages 16, 34, and 41.

[10] Shore, B. W. e P. L. Knight: *The Jaynes-Cummings Model*. J. of Mod. Opt., 40:1195, 1993. Quoted 2 times on pages 16 and 41.

[11] Brus, L.E.: *Electron-electron and electron-hole interactions in small semiconductor crystallites: The size dependence of the lowest excited electronic state.* The J. of Chem. Phys., 80:4403, 1984. Quoted on the page 17.

[12] Reed, M. A., J. N. Randall, R. J. Aggarwal, R. J. Matyi, T. M. Moore e A. E. Wetsel: *Observation of discrete electronic states in a zero-dimensional semiconductor nanostructure.* Phys. Rev. Lett., 60:535, 1988. Quoted on the page 17.

[13] Warburton, R. J.: *Self-assembled semiconductor quantum dots.* Cont. Phys., 43:351, 2002. Quoted 2 times on pages 18 and 38.

[14] Landi, S. M., M. P. Pires, C. V. B. Tribuzy, P. L. Souza, E. Marega Jr., A. G. Silva e P. S. S. Guimarães: *InAs/InGaAs/InP structures for quantum dot infrared photodetectors.* Phys. Stat. Sol. c, 8:3171, 2005. Quoted on the page 18.

[15] Silva, AG, FE Lopez, PSS Guimarães, MP Pires, PL Souza, SM Landi, JM Villas-Bôas, GS Vieira, H Vinck-Posada e BA Rodriguez: *Tunneling through stacked InAs/InGaAs/InP self-assembled quantum dots in a magnetic field.* Journal of Applied Physics, 110(8):083717, 2011. Quoted on the page 18.

[16] J. Joannopoulos, R. Meade e J. Winn: *Photonic crystals: Molding the flow of light.* Princeton University press, 1995. Quoted 2 times on pages 18 and 38.

[17] Gerard, J.M., D. Barrier, J.Y. Marzin, R. Kuszelewicz, L. Manin, E. Costard, V. Thierry-Mieg e T. Rivera: *Quantum boxes as active probes for photonic microstructures:The pillar microcavity case.* Appl. Phys. Lett., 69:449, 1996. Quoted on the page 19.

[18] Akahane, Y., T. Asano, B. Song e S. Noda: *High-Q photonic nanocavity in a two-dimensional photonic crystal.* Nature, 425:944, 2003. Quoted on the page 19.

[19] Vahala, K.J.: *Optical microcavities.* Nature, 424:839, 2003. Quoted 2 times on pages 19 and 20.

[20] Hopfield, J.: *Theory of the Contribution of Excitons to the Complex Dielectric Constant of Crystals.* Phys. Rev., 112:1555, 1952. Quoted on the page 19.

[21] Weisbuch, C., M. Nishioka, A. Ishikawa e Y. Arakawa: *Observation of the coupled exciton-photon mode splitting in a semiconductor quntum microcavity.* Phys. Rev. Lett., 69:3314, 1992. Quoted on the page 19.

[22] Houdre, R., J.L. Gibernon, P. Pellandini, R.P. Stanley, U. Oesterle, C. Weisbuch, J. O'Gorman, B. Roycroft e M. Ilegems: *Saturation of the strong-coupling regime in a semiconductor Free-carrier bleaching of cavity polaritons microcavity.* Phys. Rev. B, 52:7810, 1995. Quoted on the page 19.

[23] Tartakovski, A.I., V.D. Kulakovski, Yu.I. Koval, T.B. Borzenko, A. Forchel e J.P. Reithmaier: *Exciton-photon interaction in low-dimensional semiconductor microcavities*. J. of Exp. and Theo. Phys., 87:723, 1998. Quoted on the page 20.

[24] Bloch, J., F. Boeuf, J.M. Gerard, B. Legrand, J.Y. Marzin, R. Planel, V. Thierry-Mieg e E. Costard: *Strong and weak coupling regime in pillar semiconductor microcavities*. Physica E, 2:915, 1998. Quoted on the page 20.

[25] Gutbrod, T., M. Bayer, A. Forchel, , J.P. Reithmaier, T.L. Reinecke, S. Rudin e P.A. Knipp: *Weak and strong coupling of photons and excitons in photonic dots*. Phys. Rev. B, 57:9950, 1998. Quoted on the page 20.

[26] Cao, H., S. Pau, J.M. Jacobson, G. Bjork, Y. Yamamoto e A. Imamoglu: *Transition from a microcavity exciton polariton to a photon laser*. Phys. Rev. A, 55:4632, 1997. Quoted on the page 20.

[27] Deng, Hui, Gregor Weihs, Charles Santori, Jacqueline Bloch e Yoshihisa Yamamoto: *Condensation of Semiconductor Microcavity Exciton Polaritons*. Science, 298:199, 2002. Quoted on the page 20.

[28] Gao, J., S. Combrie, B. Liand, P. Schimitterckert, G. Lehoucq, S. Xavier, X Xu, K. Busch, D. L Huffaker, A. De Rossi e C. W. Wong: *Strongly coupled slow-light polariton sin one-dimensional disordered localized states*. Scientific Report, 3:2, 2013. Quoted on the page 20.

[29] J. Perea, D. Porras e C. Tejedor: *Dynamics of the excitation of a quantum dot in microcavity*. Physical Review B, 70:115304, 2004. Quoted 2 times on pages 21 and 39.

[30] Quang, T., G.S. Agarwal, J. Bergou, M.O. Scully, H. Walther, K. Vogel e W.P. Schleich: *Calculation of the micromaser spectrum. I. Green's-function approach and approximate analytical techniques*. Phys. Rev. A, 48:803, 1993. Quoted on the page 22.

[31] Boyd, Robert W, Alexander L Gaeta e Enno Giese: *Nonlinear optics*. Springer, 2008. Quoted on the page 24.

[32] Papadopoulos, Manthos G, Andrzej J Sadlej, Jerzy Leszczynski *et al.*: *Non-linear optical properties of matter*. Springer, 2006. Quoted on the page 24.

[33] Portacio, Alfonso A, Boris A Rodríguez e Pablo Villamil: *Theoretical study on optical response in nanostructures in the Born–Markov regime: The role of spontaneous emission and dephasing*. Annals of Physics, 400:279–288, 2019. Quoted 3 times on pages 24, 25, and 26.

[34] Barnham, Keith e Dimitri Vvedensky: *Low-dimensional semiconductor structures*. Cambridge University Press, 2001. Quoted on the page 26.

[35] Brillson, LJ, GM Foster, J Cox, WT Ruane, AB Jarjour, H Gao, H Von Wenckstern, M Grundmann, B Wang, DC Look *et al.*: *Defect Characterization, Imaging, and Control in Wide-Bandgap Semiconductors and Devices*. Journal of Electronic Materials, 47:4980–4986, 2018. Quoted on the page 26.

[36] Yokogawa, Sozo: *Nanophotonics contributions to state-of-the-art CMOS Image Sensors*. Em *2019 IEEE International Electron Devices Meeting (IEDM)*, páginas 16–1. IEEE, 2019. Quoted on the page 26.

[37] Liu, Jin, Rongbin Su, Yuming Wei, Beimeng Yao, Saimon Filipe Covre da Silva, Ying Yu, Jake Iles-Smith, Kartik Srinivasan, Armando Rastelli, Juntao Li *et al.*: *A solid-state source of strongly entangled photon pairs with high brightness and indistinguishability*. Nature nanotechnology, 14(6):586–593, 2019. Quoted on the page 26.

[38] Liu, Xiaolong e Mark C Hersam: *2D materials for quantum information science*. Nature Reviews Materials, 4(10):669–684, 2019. Quoted on the page 26.

[39] Zeiri, N, A Naifar, S Abdi Ben Nasrallah e M Said: *Third nonlinear optical susceptibility of CdS/ZnS core-shell spherical quantum dots for optoelectronic devices*. Optik, 176:162–167, 2019. Quoted on the page 26.

[40] Von Helversen, Martin, Jonas Böhm, Marco Schmidt, Manuel Gschrey, Jan Hindrik Schulze, André Strittmatter, Sven Rodt, Jörn Beyer, Tobias Heindel e Stephan Reitzenstein: *Quantum metrology of solid-state single-photon sources using photon-number-resolving detectors*. New Journal of Physics, 21(3):035007, 2019. Quoted on the page 26.

[41] Loss, Daniel e David P DiVincenzo: *Quantum computation with quantum dots*. Physical Review A, 57(1):120, 1998. Quoted on the page 26.

[42] Phillips, Jamie: *Evaluation of the fundamental properties of quantum dot infrared detectors*. Journal of Applied Physics, 91(7):4590–4594, 2002. Quoted on the page 26.

[43] Li, Ludong, Leilei Gu, Zheng Lou, Zhiyong Fan e Guozhen Shen: *ZnO quantum dot decorated Zn2SnO4 nanowire heterojunction photodetectors with drastic performance enhancement and flexible ultraviolet image sensors*. ACS nano, 11(4):4067–4076, 2017. Quoted on the page 26.

[44] Bimberg, D, N Kirstaedter, NN Ledentsov, Zh I Alferov, PS Kop'Ev e VM Ustinov: *InGaAs-GaAs quantum-dot lasers*. IEEE Journal of selected topics in quantum electronics, 3(2):196–205, 1997. Quoted on the page 26.

[45] Ye, Shuai, Jiaqing Guo, Jun Song e Junle Qu: *Achieving high-resolution of 21 nm for STED nanoscopy assisted by CdSe@ ZnS quantum dots*. Applied Physics Letters, 116(4), 2020. Quoted on the page 26.

[46] Wang, Shalong, Zhengfeng Zhu, Yousheng Zou, Yuhang Dong, Shuting Liu, Jie Xue, Leimeng Xu, Yuhui Dong e Jizhong Song: *A low-dimension structure strategy for flexible photodetectors based on perovskite nanosheets/ZnO nanowires with broadband photoresponse*. Science China Materials, 63(1):100–109, 2019. Quoted on the page 26.

[47] Bahramiyan, Hossein: *Strain effect on the third-harmonic generation of a two-dimensional GaAs quantum dot in the presence of magnetic field and spin–orbit interaction*. Indian Journal of Physics, 94(6):789–796, 2020. Quoted on the page 26.

[48] Choubani, M, H Maaref e F Saidi: *Nonlinear optical properties of lens-shaped core/shell quantum dots coupled with a wetting layer: effects of transverse electric field, pressure, and temperature*. Journal of Physics and Chemistry of Solids, 138:109226, 2020. Quoted on the page 26.

[49] Breuer, Heinz Peter e Francesco Petruccione: *The theory of open quantum systems*. Oxford University Press on Demand, 2002. Quoted 4 times on pages 27, 34, 35, and 41.

[50] Quesada, Nicolás, Herbert Vinck-Posada e Boris A Rodríguez: *Density operator of a system pumped with polaritons: A Jaynes–Cummings-like approach*. Journal of Physics: Condensed Matter, 23(2):025301, 2010. Quoted on the page 27.

[51] Perea, JI, D Porras e C Tejedor: *Dynamics of the excitations of a quantum dot in a microcavity*. Physical Review B—Condensed Matter and Materials Physics, 70(11):115304, 2004. Quoted on the page 27.

[52] Rosencher, E e Ph Bois: *Model system for optical nonlinearities: asymmetric quantum wells*. Physical Review B, 44(20):11315, 1991. Quoted on the page 29.

[53] Portacio, Alfonso A, Boris A Rodríguez e Pablo Villamil: *Influence of the position of a donor impurity on the second-order nonlinear optical susceptibility in a cylindrical quantum dot*. Superlattices and Microstructures, 113:550–557, 2018. Quoted on the page 30.

[54] Priolo, Francesco, Tom Gregorkiewicz, Matteo Galli e Thomas F Krauss: *Silicon nanostructures for photonics and photovoltaics.* Nature nanotechnology, 9(1):19–32, 2014. Quoted on the page 30.

[55] Sahrai, M, SH Asadpour e R Sadighi-Bonabi: *Optical bistability via quantum interference from incoherent pumping and spontaneous emission.* Journal of Luminescence, 131(11):2395–2399, 2011. Quoted on the page 31.

[56] Chen, Yu Yuan, Zhuan Zhuan Liu e Ren Gang Wan: *Electromagnetically induced two-dimensional grating assisted by incoherent pump.* Physics Letters A, 381(16):1362–1368, 2017. Quoted on the page 31.

[57] Daudin, B, F Widmann, G Feuillet, Y Samson, M Arlery e JL Rouvière: *Stranski-Krastanov growth mode during the molecular beam epitaxy of highly strained GaN.* Physical Review B, 56(12):R7069, 1997. Quoted on the page 33.

[58] Yamaguchi, Koichi Yamaguchi Koichi, Kunihiko Yujobo Kunihiko Yujobo e Toshiyuki Kaizu Toshiyuki Kaizu: *Stranski-Krastanov growth of InAs quantum dots with narrow size distribution.* Japanese journal of applied physics, 39(12A):L1245, 2000. Quoted on the page 33.

[59] Yoffe, Abraham D: *Semiconductor quantum dots and related systems: electronic, optical, luminescence and related properties of low dimensional systems.* Advances in physics, 50(1):1–208, 2001. Quoted on the page 33.

[60] Dupuis, Russell D, PD Dapkus, Nick Holonyak, EA Rezek e R Chin: *Room-temperature laser operation of quantum-well Ga (1- x) AlxAs-GaAs laser diodes grown by metalorganic chemical vapor deposition.* Applied Physics Letters, 32(5):295–297, 1978. Quoted on the page 33.

[61] Butcher, Paul N, Norman H March e Mario P Tosi: *Physics of low-dimensional semiconductor structures.* Springer Science & Business Media, 2013. Quoted on the page 33.

[62] Joannopoulos, John D, Steven G Johnson, Joshua N Winn e Robert D Meade: *Molding the flow of light.* Princet. Univ. Press. Princeton, NJ [ua], 12, 2008. Quoted on the page 33.

[63] Vahala, Kerry J.: *Optical microcavities.* Nature, 424(6950):839–846, 2003. Quoted 2 times on pages 33 and 38.

[64] Gérard, Jean Michel e Bruno Gayral: *InAs quantum dots: artificial atoms for solid-state cavity-quantum electrodynamics.* Physica E: Low-dimensional Systems and Nanostructures, 9(1):131–139, 2001. Quoted on the page 33.

[65] Weisbuch, Claude, Mr Nishioka, A Ishikawa e Y Arakawa: *Observation of the coupled exciton-photon mode splitting in a semiconductor quantum microcavity.* Physical review letters, 69(23):3314, 1992. Quoted on the page 33.

[66] Warburton, Richard J.: *Self-assembled semiconductor quantum dots.* Contemporary Physics, 43(5):351–364, 2002. Quoted on the page 33.

[67] Reithmaier, J.P., G. Sęk, A. Löffler, C. Hofmann, S. Kuhn, S. Reitzenstein, L.V. Keldysh, V.D. Kulakovskii, T.L. Reinecke e A. Forchel: *Strong coupling in a single quantum dot–semiconductor microcavity system.* Nature, 432(7014):197–200, 2004. Quoted 3 times on pages 33, 39, and 40.

[68] Yoshie, Tomoyuki, Axel Scherer, J. Hendrickson, Galina Khitrova, H.M. Gibbs, G. Rupper, C. Ell, O.B. Shchekin e D.G. Deppe: *Vacuum Rabi splitting with a single quantum dot in a photonic crystal nanocavity.* Nature, 432(7014):200–203, 2004. Quoted 2 times on pages 33 and 39.

[69] Solomon, Glenn S, Matthew Pelton e Y Yamamoto: *Microcavity modified spontaneous emission of single quantum dots.* physica status solidi (b), 244(8):2792–2802, 2007. Quoted on the page 33.

[70] Hennessy, Kevin, Antonio Badolato, Martin Winger, Dario Gerace, Mete Atatüre, S Gulde, S Fält, Evelyn L Hu e A Imamoğlu: *Quantum nature of a strongly coupled single quantum dot–cavity system.* Nature, 445(7130):896–899, 2007. Quoted on the page 33.

[71] Di, Ziyun, Helene V Jones, Philip R Dolan, Simon M Fairclough, Matthew B Wincott, Johnny Fill, Gareth M Hughes e Jason M Smith: *Controlling the emission from semiconductor quantum dots using ultra-small tunable optical microcavities.* New Journal of Physics, 14(10):103048, 2012. Quoted on the page 33.

[72] Kim, Hyochul, Thomas C Shen, Deepak Sridharan, Glenn S Solomon e Edo Waks: *Magnetic field tuning of a quantum dot strongly coupled to a photonic crystal cavity.* Applied Physics Letters, 98(9), 2011. Quoted 2 times on pages 34 and 36.

[73] O'brien, Jeremy L, Akira Furusawa e Jelena Vučković: *Photonic quantum technologies.* Nature Photonics, 3(12):687–695, 2009. Quoted on the page 34.

[74] Michler, Peter, Alper Kiraz, Christoph Becher, WV Schoenfeld, PM Petroff, Lidong Zhang, Ella Hu e A Imamoglu: *A quantum dot single-photon turnstile device.* science, 290(5500):2282–2285, 2000. Quoted on the page 34.

[75] Carmichael, Howard J: *Statistical methods in quantum optics 1: master equations and Fokker-Planck equations.* Springer Science & Business Media, 2013. Quoted 2 times on pages 34 and 35.

[76] Scully, Marlan O e M Suhail Zubairy: *Quantum optics*. Cambridge university press, 1997. Quoted 2 times on pages 34 and 35.

[77] Johansson, J Robert, Paul D Nation e Franco Nori: *QuTiP: An open-source Python framework for the dynamics of open quantum systems*. Computer physics communications, 183(8):1760–1772, 2012. Quoted on the page 35.

[78] Bastard, G.: *Wave mechanics applied to semiconductor heterostructures*. John Wiley and Sons Inc., 1990. Quoted on the page 38.

[79] Haug, Hartmut e Stephan W. Koch: *Quantum theory of the optical and electronic properties of semiconductors*. World Scientific Publishing Company, 2009. Quoted on the page 38.

[80] C. Weisbuch, H. Benisty e R. Houdre: *Overview of fundamentals and application of electrons, excitons and photons in confined structures*. J. of Luminescence., 85:271, 2000. Quoted on the page 38.

[81] Fox, A.M.: *Optoelectronics in quantum well structures*. Contemporary Physics., 37:111, 1996. Quoted on the page 38.

[82] Y. Yamamoto, F. Tassone e H. Cao: *Semiconductor cavity quantum electrodynamics*. Springer, 2000. Quoted on the page 38.

[83] Gérard, Jean Michel e Bruno Gayral: *InAs quantum dots: artificial atoms for solid-state cavity-quantum electrodynamics*. Physica E: Low-dimensional Systems and Nanostructures, 9(1):131–139, 2001. Quoted on the page 38.

[84] Mowbray, D. J. e M. S. Skolnick: *New physics and devices based on self-assembled semiconductor quantum dots*. Journal of Physics D, 38:2059, 2005. Quoted on the page 38.

[85] Ozbay, Ekmel e Mehmet Bayindir: *Physics and applications of defect structures in photonic crystals*. Em *Quantum Communication and Information Technologies*, páginas 273–297. Springer, 2003. Quoted on the page 38.

[86] Solomon, G.S., M. Pelton e Y. Yamamoto: *Modification of spontaneous emission of a single quantum dot*. Physica Status Solidi (a), 178(1):341–344, 2000. Quoted on the page 38.

[87] Kiraz, A, P Michler, C Becher, B Gayral, A Imamoğlu, Lidong Zhang, E Hu, WV Schoenfeld e PM Petroff: *Cavity-quantum electrodynamics using a single InAs quantum dot in a microdisk structure*. Applied Physics Letters, 78(25):3932–3934, 2001. Quoted on the page 38.

[88] Andreani, Lucio Claudio, Giovanna Panzarini e Jean Michel Gérard: *Strong-coupling regime for quantum boxes in pillar microcavities: Theory.* Physical Review B, 60(19):13276, 1999. Quoted on the page 38.

[89] Reitzenstein, S., C. Hofmann, A. Löffler, A. Kubanek, J.P. Reithmaier, M. Kamp, V.D. Kulakovskii, L.V. Keldysh, T.L. Reinecke e A. Forchel: *Strong and weak coupling of single quantum dot excitons in pillar microcavities.* Physica Status Solidi (b), 243(10):2224–2228, 2006. Quoted on the page 38.

[90] Reitzenstein, S., A. Loffler, C. Hofmann, A. Kubanek, M. Kamp, J.P. Reithmaier, A. Forchel, V.D. Kulakovskii, L.V. Keldysh, I.V. Ponomarev e T.L. Reinecke: *Coherent photonic coupling of semiconductor quantum dots.* Opt. Lett., 31:1738, 2006. Quoted on the page 38.

[91] Laussy, Fabrice P., Elena del Valle e Carlos Tejedor: *Strong Coupling of Quantum Dots in Microcavities.* Phys. Rev. Lett., 101:083601, Aug 2008. Quoted 3 times on pages 39, 43, and 50.

[92] Del Valle, Elena e F.P. Laussy: *Regimes of strong light-matter coupling under incoherent excitation.* Physical Review A, 84(4):043816, 2011. Quoted 2 times on pages 39 and 50.

[93] Roy, C e S Hughes: *Master equations for semiconductor cavity-QED.* Em *AIP Conference Proceedings*, volume 1398, páginas 33–37. American Institute of Physics, 2011. Quoted on the page 39.

[94] Jiménez-Orjuela, C.A., H. Vinck-Posada e José M. Villas-Bôas: *Strong coupling of two quantum dots with a microcavity in the presence of an external and tilted magnetic field.* Physica B: Condensed Matter, 585:412070, 2020. Quoted on the page 39.

[95] Poddubny, A.N., M.M. Glazov e N.S. Averkiev: *Nonlinear emission spectra of quantum dots strongly coupled to a photonic mode.* Physical Review B, 82(20):205330, 2010. Quoted 3 times on pages 39, 41, and 50.

[96] Valle, Elena del: *Strong and weak coupling of two coupled qubits.* Physical Review A, 81(05):053811, 2010. Quoted on the page 39.

[97] Bradley, A.L., J.P. Doran, T. Aherne, J. Hegarty, R.P. Stanley, R. Houdré, U. Oesterle e M. Ilegems: *Nonlinear reflectivity of semiconductor microcavities in the weak-and strong-coupling regimes: Experiment and theory.* Physical Review B, 57(16):9957, 1998. Quoted on the page 39.

[98] Gutbrod, T., M. Bayer, A. Forchel, J.P. Reithmaier, T.L. Reinecke, S. Rudin e P.A. Knipp: *Weak and strong coupling of photons and excitons in photonic dots.* Physical Review B, 57(16):9950, 1998. Quoted on the page 39.

[99] Bloch, J., F. Boeuf, J.M. Gérard, B. Legrand, J.Y. Marzin, R. Planel, V. Thierry-Mieg e E. Costard: *Strong and weak coupling regime in pillar semiconductor microcavities.* Physica E: Low-dimensional Systems and Nanostructures, 2(1-4):915–919, 1998. Quoted on the page 39.

[100] Obert, M., J. Renner, A. Forchel, G. Bacher, Régis André e D. Le Si Dang: *Nonlinear emission in II–VI pillar microcavities: Strong versus weak coupling.* Applied Physics Letters, 84(9):1435–1437, 2004. Quoted on the page 39.

[101] Nikolaev, N.I., A. Smith e A.L. Ivanov: *Polariton optics of semiconductor photonic dots: weak and strong coupling limits.* Journal of Physics: Condensed Matter, 16(35):S3703, 2004. Quoted on the page 39.

[102] Inoue, Jun ichi, Tetsuyuki Ochiai e Kazuaki Sakoda: *Emission spectra from a high Q weak coupling system.* Journal of the Physical Society of Japan, 75(9):094720–094720, 2006. Quoted on the page 39.

[103] Bilykh, V.V., M.H. Nguyen, N.N. Sibeldin, M.L. Skorikov, V.A. Tsvetkov e A.V. Sharkov: *Dynamics of the transition from strong to weak coupling regime in a system of exciton polaritons in semiconductor microcavities.* Journal of Experimental and Theoretical Physics, 109(3):472–479, 2009. Quoted on the page 39.

[104] Lin, Hsuan, Chia Hsien Lin, Wei Chen Lai, Yi Shan Lee, Sheng Di Lin e Wen Hao Chang: *Stress tuning of strong and weak couplings between quantum dots and cavity modes in microdisk microcavities.* Physical Review B, 84(20):201301, 2011. Quoted on the page 39.

[105] Zhang, J.S., L. Chen, M. Abdel-Aty e A.X. Chen: *Sudden death and robustness of quantum correlations in the weak-or strong-coupling regime.* The European Physical Journal D, 66(1):1–8, 2012. Quoted on the page 39.

[106] Hümmer, Thomas, F.J. García-Vidal, Luis Martín-Moreno e David Zueco: *Weak and strong coupling regimes in plasmonic QED.* Physical Review B, 87(11):115419, 2013. Quoted on the page 39.

[107] Rodriguez, S.R.K., Y.T. Chen, T.P. Steinbusch, M.A. Verschuuren, A.F. Koenderink e J. Gómez Rivas: *From weak to strong coupling of localized surface plasmons to guided modes in a luminescent slab.* Physical Review B, 90(23):235406, 2014. Quoted on the page 39.

[108] Reitzenstein, S. e A. Forchel: *Quantum dot micropillars.* J. Phys. D: Appl. Phys., 43:25, 2010. Quoted 2 times on pages 40 and 41.

[109] Carmichael, Howard: *Statistical methods in quantum optics 1: master equations and Fokker-Planck equations*, volume 1. Springer Science & Business Media, 1999. Quoted 2 times on pages 41 and 42.

[110] Carmichael, Howard: *An open systems approach to quantum optics: lectures presented at the Université Libre de Bruxelles, October 28 to November 4, 1991*, volume 18. Springer Science & Business Media, 2009. Quoted on the page 41.

[111] Laussy, Fabrice P., Elena Del Valle e Carlos Tejedor: *Luminescence spectra of quantum dots in microcavities. I. Bosons.* Physical Review B, 79(23):235325, 2009. Quoted on the page 41.

[112] Yao, Peijun, PK Pathak, E Illes, S Hughes, S Münch, S Reitzenstein, P Franeck, A Löffler, T Heindel, S Höfling *et al.*: *Nonlinear photoluminescence spectra from a quantum-dot–cavity system: Interplay of pump-induced stimulated emission and anharmonic cavity QED.* Physical Review B, 81(3):033309, 2010. Quoted on the page 41.

[113] Tian, L e HJ Carmichael: *Incoherent excitation of the Jaynes-Cummings system.* Quantum Optics: Journal of the European Optical Society Part B, 4(2):131, 1992. Quoted on the page 41.

[114] Laucht, A., N. Hauke, J.M. Villas-Bôas, F. Hofbauer, G. Böhm, M. Kaniber e J.J. Finley: *Dephasing of exciton polaritons in photoexcited InGaAs quantum dots in GaAs nanocavities.* Physical Review Letters, 103(8):087405, 2009. Quoted 2 times on pages 42 and 44.

[115] Valle, Elena del, Fabrice P. Laussy e Carlos Tejedor: *Luminescence spectra of quantum dots in microcavities. II. Fermions.* Physical Review B, 79:235326, Jun 2009. Quoted on the page 44.

[116] Gayral, B. e J.M. Gérard: *Photoluminescence experiment on quantum dots embedded in a large Purcell-factor microcavity.* Physical Review B, 78(23):235306, 2008. Quoted on the page 50.

[117] Vera, Carlos A., Nicolás Quesada, Herbert Vinck-Posada e Boris A. Rodríguez: *Characterization of dynamical regimes and entanglement sudden death in a microcavity quantum dot system.* Journal of Physics: Condensed Matter, 21(39):395603, 2009. Quoted on the page 50.

[118] Tarel, Guillaume e Vincenzo Savona: *Linear spectrum of a quantum dot coupled to a nanocavity.* Physical Review B, 81(7):075305, 2010. Quoted on the page 50.

[119] Rivera, Nicholas e Ido Kaminer: *Light–matter interactions with photonic quasiparticles*. Nature Reviews Physics, 2(10):538–561, 2020. Quoted on the page 50.